



A numerical study of the Dirac Spectrum and Transmission Problems employing the Method of Fundamental Solutions

Francisco Alves Bento

Thesis to obtain the Master of Science Degree in

Applied Mathematics and Computation

Supervisors: Pedro Ricardo Simão Antunes
Juha Hans Videman

Examination Committee

Chairperson: Prof. Pedro Lima
Members of the Committee: Prof. Hugo Tavares
Prof. Pedro Serranho

September 2023

“Thinking is learning all over again
how to see, directing one’s
consciousness, making of every
image a privileged place.”

Albert Camus
The Myth of Sisyphus

Acknowledgments

I would like to thank my parents for their friendship, encouragement and caring over all these years, for always being there for me through thick and thin and without whom this project would not be possible. I would also like to thank my grandparents, aunts, uncles and cousins for their understanding and support throughout all these years.

Quisque facilisis erat a dui. Nam malesuada ornare dolor. Cras gravida, diam sit amet rhoncus ornare, erat elit consectetur erat, id egestas pede nibh eget odio. Proin tincidunt, velit vel porta elementum, magna diam molestie sapien, non aliquet massa pede eu diam. Aliquam iaculis.

Fusce et ipsum et nulla tristique facilisis. Donec eget sem sit amet ligula viverra gravida. Etiam vehicula urna vel turpis. Suspendisse sagittis ante a urna. Morbi a est quis orci consequat rutrum. Nullam egestas feugiat felis. Integer adipiscing semper ligula. Nunc molestie, nisl sit amet cursus convallis, sapien lectus pretium metus, vitae pretium enim wisi id lectus.

Donec vestibulum. Etiam vel nibh. Nulla facilisi. Mauris pharetra. Donec augue. Fusce ultrices, neque id dignissim ultrices, tellus mauris dictum elit, vel lacinia enim metus eu nunc.

I would also like to acknowledge my dissertation supervisors Prof. Some Name and Prof. Some Other Name for their insight, support and sharing of knowledge that has made this Thesis possible.

Last but not least, to all my friends and colleagues that helped me grow as a person and were always there for me during the good and bad times in my life. Thank you.

To each and every one of you – Thank you.

Abstract

Nulla facilisi. In vel sem. Morbi id urna in diam dignissim feugiat. Proin molestie tortor eu velit. Aliquam erat volutpat. Nullam ultrices, diam tempus vulputate egestas, eros pede varius leo, sed imperdiet lectus est ornare odio. Lorem ipsum dolor sit amet, consectetur adipiscing elit. Proin consectetur velit in dui. Phasellus wisi purus, interdum vitae, rutrum accumsan, viverra in, velit. Sed enim risus, congue non, tristique in, commodo eu, metus. Aenean tortor mi, imperdiet id, gravida eu, posuere eu, felis. Mauris sollicitudin, turpis in hendrerit sodales, lectus ipsum pellentesque ligula, sit amet scelerisque urna nibh ut arcu. Aliquam in lacus. Vestibulum ante ipsum primis in faucibus orci luctus et ultrices posuere cubilia Curae; Nulla placerat aliquam wisi. Mauris viverra odio. Quisque fermentum pulvinar odio. Proin posuere est vitae ligula. Etiam euismod. Cras a eros.

Keywords

Maecenas tempus dictum libero; Donec non tortor in arcu mollis feugiat; Cras rutrum pulvinar tellus.

Resumo

Pellentesque habitant morbi tristique senectus et netus et malesuada fames ac turpis egestas. Vestibulum tortor quam, feugiat vitae, ultricies eget, tempor sit amet, ante. Donec eu libero sit amet quam egestas semper. Aenean ultricies mi vitae est. Mauris placerat eleifend leo. Quisque sit amet est et sapien ullamcorper pharetra. Vestibulum erat wisi, condimentum sed, commodo vitae, ornare sit amet, wisi. Aenean fermentum, elit eget tincidunt condimentum, eros ipsum rutrum orci, sagittis tempus lacus enim ac dui. Donec non enim in turpis pulvinar facilisis. Ut felis. Aliquam aliquet, est a ullamcorper condimentum, tellus nulla fringilla elit, a iaculis nulla turpis sed wisi. Fusce volutpat. Etiam sodales ante id nunc. Proin ornare dignissim lacus. Nunc porttitor nunc a sem. Sed sollicitudin velit eu magna. Aliquam erat volutpat. Vivamus ornare est non wisi. Proin vel quam. Vivamus egestas. Nunc tempor diam vehicula mauris. Nullam sapien eros, facilisis vel, eleifend non, auctor dapibus, pede.

Palavras Chave

Colaborativo; Codificação; Conteúdo Multimídia; Comunicação;

Contents

1	Introduction	1
1.1	Thesis Overview	2
2	Some Preliminary Results	3
2.1	Some concepts on Banach Spaces	4
2.2	Some concepts on Hilbert Spaces	8
2.3	Lebesgue and Sobolev Spaces	12
2.4	Spectral Decomposition of the Laplace Operator	17
3	From Spectral Theory to Geometry and Shape Optimization	21
3.1	The Laplace Operator	22
3.2	The Dirac Operator	25
3.3	A domain decomposition problem	31
4	The Method of Fundamental Solutions	39
4.1	Density and linear independence results	40
4.2	Numerical approach for the Laplace Equation	47
4.2.1	An enrichment technique	49
4.3	Numerical approach for the Helmholtz Equation	52
4.3.1	The Subspace Angle Technique	53
5	Conducted Numerical Simulations	55
5.1	Poisson Equation using MFS-B	56
5.2	Poisson Equation using MFS-D	57
5.3	Helmholtz Equation using MFS-B	57
5.3.1	User Interface	58
5.3.2	Vivamus luctus elit sit amet mi	58
5.4	Helmholtz Equation in Rectangular Domains using MFS-B	60
5.5	Helmholtz Equation in Rectangular Domains using MFS-D	60
5.6	Dirac Operator Spectrum in Rectangular Domains using MFS-B	60
5.7	Dirac Operator Spectrum in Rectangular Domains using MFS-D	60

5.8 Dirac Operator Spectrum in General Polygonal Domains using MFS-D	60
6 The Poisson Equation with Variable Coefficients	61
6.1 Maecenas vitae nulla consequat	62
6.2 Proin ornare dignissim lacus	63
7 Conclusion	65
7.1 Conclusions	66
7.2 System Limitations and Future Work	67
Bibliography	69
Glossary	73
A Code of Project	75
B A Large Table	83

List of Figures

3.1	A wedge domain with an interior angle θ .	30
4.1	A wedge domain with an interior angle Θ .	49
4.2	Rotation of the wedge domain. Image taken from [1].	51
5.1	Complete User Interface	59
6.1	Test Environment	62
6.2	Adaptation System Behavior Test	64

List of Tables

6.1	Network Link Conditioner Profiles	63
B.1	Example table	84
B.2	Example of a very long table spreading in several pages	84
B.3	Sample Table.	86

List of Algorithms

5.1 Time Control Strategy	57
-------------------------------------	----

Listagens

5.1	A listing with a Tikz picture overlayed	58
A.1	Example of a XML file.	75
A.2	Assembler Main Code.	76
A.3	Matlab Function	77
A.4	function.m	78
A.5	HTML with CSS Code	78
A.6	HTML CSS Javascript Code	80
A.7	PYTHON Code	81

Acronyms

UI User Interface

1

Introduction

Contents

1.1 Thesis Overview	2
-------------------------------	---

Partial Differential Equations (PDEs) are one of the most powerful mathematical techniques in mathematical modelling, with direct applications in engineering, physics and even machine learning. As such, the development of reliable numerical methods to solve them are of major importance since most of these equations cannot be solved analytically. Throughout this work we are going to explore a newly developed class type of numerical methods known as *meshless* or *meshfree* methods and its applications in open problems in mathematical-physics. Contrary to the widely used classical methods like finite differences and finite element methods which involve some previously created mesh (where numerically solving a PDE might be difficult if the domain's geometry is convoluted), these type of meshless methods are easier to use since they are mostly independent from the domain, at least from an implementation point of view.

The meshless method we are interested in is known as the Method of Fundamental Solutions (MFS) that is based on the fundamental solutions of well-known equations such as the Laplace Equation and the Helmholtz equation. As we are going to see, such set of functions have some interesting properties that we can use to numerically solve PDEs. We are also going to implement a generalization of MFS based on *Kansa method*, another meshless method that in turn uses radial basis functions.

One of the main points of this work is to address open conjectures related with the spectrum of the Dirac Operator while seeking numerical evidence of some proposed isoperimetric inequalities using the methods listed above. Motivated by developments in molecular and nuclear physics, and the particularly interesting properties of low energy charge carriers in graphene, Dirac equation replaced the non-relativistic Schrödinger Equation. Unfortunately, the matrix structure found in the Dirac Equation makes it harder to study. The interest in capable numerical methods arises in such conditions: not only can they be used to test some conjectures but they can also be a source of insights for future advances.

1.1 Thesis Overview

2

Some Preliminary Results

Contents

2.1	Some concepts on Banach Spaces	4
2.2	Some concepts on Hilbert Spaces	8
2.3	Lebesgue and Sobolev Spaces	12
2.4	Spectral Decomposition of the Laplace Operator	17

2.1 Some concepts on Banach Spaces

This section begins by introducing preliminary concepts on Banach Spaces, which play a crucial role in the subsequent numerical methods to be presented. For more details see [2] or [3]. Consider a field \mathbb{F} (\mathbb{R} or \mathbb{C}). We say that a vector space E is a *normed space* if there exists a map $\|\cdot\|$ (called a *norm*) over \mathbb{F} such that

1. $\|\alpha x\| = |\alpha| \|x\|, \alpha \in \mathbb{F}, \forall x \in E$;
2. $\|x + y\| \leq \|x\| + \|y\|, \forall x, y \in E$;
3. $\|x\| \geq 0, \forall x \in E$;
4. $\|x\| = 0 \iff x = 0$.

In particular, a pivotal notion is of *Banach spaces*, i.e, E is a Banach space if it is a complete normed space.

Definition 2.1.1. Consider a linear operator $T : E \rightarrow F$, where E and F are Banach spaces with the associated norms $\|\cdot\|_E$ and $\|\cdot\|_F$, respectively. Then

1. The **nullspace** (also called the **kernel**) of T is a subset of E such that

$$N(T) = \{x \in E : Tx = 0\}.$$

Accordingly, the **range** (also called the **image**) of T is a subset of F such that

$$R(T) = \{y \in F : \text{there exists some } x \in E \text{ such that } y = Tx\}.$$

2. T is said to be **bounded** (continuous) if there exists $C > 0$ such that $\|Tx\|_F \leq C\|x\|_E$. We define the norm of the operator T as

$$\|T\| = \sup_{\substack{x \in E \\ x \neq 0}} \frac{\|Tx\|_F}{\|x\|_E}.$$

In this case we write $T \in \mathcal{L}(E, F)$. If $E = F$, we write $T \in \mathcal{L}(E)$;

3. The space of linear and continuous maps from E to \mathbb{R} is the **dual space** of E denoted by E^* . If $S \in E^*$, its norm (the dual norm) is defined in the same manner as the operator norm above, i.e.

$$\|S\| = \sup_{\substack{x \in E \\ x \neq 0}} \frac{|\langle S, x \rangle|}{\|x\|}$$

where $\langle S, x \rangle_{E^*, E} = Sx$ and denotes the duality pairing between E^* and E . As we will see below, it generalizes the notion of inner product in inner product spaces. Whenever it is obvious what dual pairing is being considered we just write $\langle \cdot, \cdot \rangle$;

4. Assuming that T is bounded, T is said to be **compact** if for any bounded sequence $(u_n)_{n \in \mathbb{N}} \subset E$ there exists a subsequence $(u_{n_k})_{k \in \mathbb{N}}$ such that $(Tu_{n_k})_{k \in \mathbb{N}}$ converges in F ;
5. Assume that the domain of T , which we represent by $\text{Dom}(T)$, is dense in E . We say that the linear operator $T^* : \text{Dom}(T^*) \subset F^* \rightarrow E^*$ is the **adjoint** of T if

$$\langle v, Tu \rangle_{F^*, F} = \langle T^*v, u \rangle_{E^*, E^*}, \quad \forall v \in \text{Dom}(T^*),$$

where the domain of T^* is defined by

$$\text{Dom}(T^*) = \{v \in F^* : \exists c \geq 0 \text{ such that } |\langle v, Tu \rangle_{F^*, F}| \leq c\|u\|, \quad \forall u \in \text{Dom}(T)\}.$$

The main result of this section concerns the dual of a normed space. In reality, we do not need to assume that E is a Banach space to present the next results. However, throughout this work, every normed space is also complete. We refer to Chapters 1 and 3 from [3].

Definition 2.1.2 (Reflexive space). *Let E be a normed space and denote its dual by E^* . The bidual space E^{**} is the dual of E^* with the associated norm*

$$\|\xi\| = \sup_{\substack{f \in E^* \\ f \neq 0}} \frac{|\langle \xi, f \rangle|}{\|f\|}.$$

If the (canonical) map $J : E \rightarrow E^{**}$ defined by

$$\langle Jx, f \rangle_{E^{**}, E^*} = \langle f, x \rangle_{E^*, E}, \quad \forall x \in E, \forall f \in E^*$$

is surjective then E is said to be reflexive.

The definition above is an important detail to the justification of the Method of Fundamental Solutions. The main ingredient to justify this numerical method is the Hahn-Banach theorem.

Theorem 2.1.3 (Analytical form of Hahn-Banach Theorem). *Let E be a normed space and $p : E \rightarrow \mathbb{R}$ a functional satisfying*

$$p(\lambda x) = \lambda p(x), \quad \forall x \in E, \quad \lambda > 0$$

$$p(x + y) \leq p(x) + p(y)$$

Let $G \subset E$ be a linear subspace and $g : G \rightarrow \mathbb{R}$ a linear functional such that

$$g(x) \leq p(x), \forall x \in G.$$

Then, there exists a linear functional $f : E \rightarrow \mathbb{R}$ that extends g to E , agrees with g on G , i.e, $f(x) = g(x)$, $\forall x \in G$ and also satisfies

$$f(x) \leq p(x) \forall x \in E.$$

Remark 2.1.4. The theorem mentioned above holds particular significance in Functional Analysis as it demonstrates that the dual E^* of a normed space E possesses interesting properties that warrant further study to gain a better understanding of the underlying space E . It can even be utilized to identify, although not uniquely, elements in both E and its dual E^* through the duality pairing. This result bears resemblance to the desirable properties exhibited by Hilbert spaces, which we will explore further in this work. It is beneficial to establish density when working with the dual pairing between a Banach space and its dual. However, it is important to note that the existence of the functional f is not explicitly provided, as the proof of Theorem (2.1.3) relies on the Axiom of Choice (Zorn's Lemma).

Under some conditions, an interesting consequence of Theorem (2.1.3) is that two disjoint (and non-empty) convex sets can always be separated by a hyperplane in an infinite-dimensional space.

Definition 2.1.5. Let E be a normed space, f a linear functional on E , and $c \in \mathbb{R}$. An hyperplane H is a subset of E of the form

$$H = \{x \in E : \langle f, x \rangle = c\}.$$

Proposition 2.1.6. Let H be a hyperplane defined by the equation $\langle f, x \rangle = c$, for some linear functional f and $c \in \mathbb{R}$. Then, H is closed if and only if f is continuous.

Notice that if H is a closed hyperplane then the linear functional f that defines the hyperplane is an element of E^* .

Definition 2.1.7. Let A and B be two subsets of E . We say that a hyperplane H defined by the equation $\langle f, x \rangle = c$, for some linear functional f and $c \in \mathbb{R}$, strictly separates A and B if

$$\langle f, x \rangle < c, \forall x \in A,$$

$$\langle f, x \rangle > c, \forall x \in B$$

Theorem 2.1.8 (Second geometric form of Hahn-Banach Theorem). Let A and B be two disjoint, non-empty and convex subsets of E such that A is closed and B is compact. Then, there exists a closed hyperplane that strictly separates A and B , i.e, there exists $f \in E^*$ and $c \in \mathbb{R}$ such that for every $a \in A$

and $b \in B$

$$\langle f, a \rangle < c < \langle f, b \rangle.$$

The following Lemma is a consequence of Theorem (2.1.8), and it is a useful tool to prove that some linear subspace $M \subset E$ is dense (in E). We start by introducing the notion of orthogonality of sets in Banach spaces with respect to the duality pairing.

Definition 2.1.9. *Let E be a Banach Space and M be a linear subspace of E . We define the orthogonal of M in E with respect to the duality pairing as*

$$M^\perp = \{\psi \in E^* : \langle \psi, \varphi \rangle = 0, \forall \varphi \in M\}.$$

Accordingly, if $N \subset E^*$ is a linear subspace, its orthogonal is defined as

$$N^\perp = \{\varphi \in E : \langle \psi, \varphi \rangle = 0, \forall \psi \in N\}$$

Lemma 2.1.10. *Let M and N in the same conditions of the definition above. Then*

$$(M^\perp)^\perp = \overline{M}$$

and

$$\overline{N} \subset (N^\perp)^\perp.$$

In particular, if E is a reflexive Banach space then

$$(N^\perp)^\perp = \overline{N}.$$

Proof. Since $(M^\perp)^\perp \subset E$ and $(N^\perp)^\perp \subset E^*$ are closed sets, by definition $M \subset (M^\perp)^\perp$ and $N \subset (N^\perp)^\perp$ the inclusions

$$\overline{M} \subseteq (M^\perp)^\perp, \quad \overline{N} \subseteq (N^\perp)^\perp$$

follow. To check that $(M^\perp)^\perp \subseteq \overline{M}$ we argue by contradiction. Let $x_0 \in (M^\perp)^\perp$ such that $x_0 \notin \overline{M}$. Then, by Theorem (2.1.8) there exists a hyperplane with equation $\langle f, x \rangle = c$ for some $f \in E^*$ and $c \in \mathbb{R}$ that strictly separates the sets $\{x_0\}$ and \overline{M} (both are obviously non-empty convex sets). In particular,

$$\langle f, x \rangle_{E^*, E} < c < \langle f, x_0 \rangle_{E^*, E}, \forall x \in M.$$

Since M is a linear subspace, then $\langle f, x \rangle = 0, \forall x \in M$ since, otherwise, given any $x \in M$ we would

have that

$$\alpha \langle f, x \rangle_{E^*, E} = \langle f, \alpha x \rangle_{E^*, E} < c, \forall \alpha \in \mathbb{R}$$

which can only be possible if $\langle f, x \rangle_{E^*, E} = 0$. Therefore, $f \in M^\perp$ and $\langle f, x_0 \rangle_{E^*, E} > 0$ but that is a contradiction since, by hypothesis, $x_0 \in (M^\perp)^\perp$ and $\langle f, x_0 \rangle_{E^*, E} = 0, \forall f \in M^\perp$.

To prove that $(N^\perp)^\perp = \overline{N}$, we use the same type of argument. Let $f_0 \in (N^\perp)^\perp$ such that $f_0 \notin \overline{N}$. Once again, there exists a hyperplane with equation $\langle \xi, f \rangle = c$ for some $\xi \in E^{**}$ and $c \in \mathbb{R}$ that strictly separates $\{f_0\}$ and \overline{N} , that is

$$\langle \xi, f \rangle < c < \langle \xi, f_0 \rangle, \forall f \in N.$$

Since N is a linear subspace we can also conclude that $\langle \xi, f \rangle = 0, \forall f \in N$ and $\langle \xi, f_0 \rangle > 0$. In order to get a contradiction, like in the case above, since E is a reflexive space, then the canonical map J defined in (2.1.2) is surjective, and we can write

$$\langle \xi, f_0 \rangle_{E^{**}, E^*} = \langle Jx_0, f_0 \rangle_{E^{**}, E^*} = \langle f_0, x_0 \rangle_{E^*, E}$$

for some $x_0 \in E$. If we can prove that $\langle f_0, x_0 \rangle_{E^*, E} = 0$, then the contradiction follows. Since $f_0 \in (N^\perp)^\perp$, then $\langle f_0, x_0 \rangle_{E^*, E} = 0$ if $x_0 \in N^\perp$, i.e., $\langle f, x_0 \rangle_{E^*, E} = 0, \forall f \in N$. Let $f \in N$. Then, by reflexivity,

$$\langle f, x_0 \rangle_{E^*, E} = \langle Jx_0, f \rangle_{E^{**}, E^*} = \langle \xi, f \rangle_{E^{**}, E^*} = 0, \forall f \in N$$

as we saw above (N is a linear subspace). The desired result follows. \square

Remark 2.1.11. *The result above will be useful to justify the Method of Fundamental Solutions. To prove that some subset N of a Banach Space E is dense it will suffice to show that its orthogonal N^\perp only contains the trivial element, which belongs to both E and E^* .*

2.2 Some concepts on Hilbert Spaces

In this section we introduce some complementary results in Hilbert spaces. Once again, for more details, see [2], [3] or [4]. Consider the field \mathbb{F} (\mathbb{R} or \mathbb{C}). We say that a vector space H is an *inner product space* (or a Pre-Hilbert space) if there exists a map (\cdot, \cdot) (called an *inner product*) over \mathbb{F} such that

1. $(x, y) = \overline{(y, x)}$ (The bar denotes complex conjugation if $\mathbb{F} = \mathbb{C}$);
2. $(x + y, z) = (x, z) + (y, z)$;
3. $(\alpha x, y) = \alpha(x, y), \alpha \in \mathbb{F}$;
4. $(x, x) \geq 0, \forall x \in H$;

$$5. (x, x) = 0 \iff x = 0.$$

Given $x, y \in H$, we say that x and y are orthogonal (denoted by $x \perp y$) if $(x, y) = 0$. Accordingly, given $E, F \subset H$, if $x \perp y$ for every $x \in E, y \in F$ then we say that E and F are orthogonal, $E \perp F$. We also denote by E^\perp the set of all $y \in H$ that are orthogonal to every $x \in E$, i.e, $E^\perp = \{y \in H : (x, y) = 0, \forall x \in E\}$ which we call the orthogonal complement of E . We recall that every inner product space is also a normed space, where the inner product induces the norm

$$\|x\| = \sqrt{(x, x)}$$

satisfying the Cauchy-Schwarz inequality

$$|(x, y)| \leq \|x\| \|y\|, \quad x, y \in H.$$

Finally, if the normed space is complete for the induced norm, then we say that it is a Hilbert space. In what follows, H will always denote a Hilbert space.

Example 2.2.1. A very classical Hilbert space, which is going to be used throughout all of this work, is the space of square-integrable real-valued functions in an open and bounded subset Ω of \mathbb{R}^d , which is denoted by $L^2(\Omega)$ with the inner product given by

$$(f, g)_{L^2(\Omega)} = \int_{\Omega} f(x)g(x)dx.$$

While working within the framework of Hilbert spaces, proving the density of a subspace $M \subset H$ is more intuitive and can be derived straightforwardly. It may be of interest to the reader to compare the following results with Definition (2.1.9) and Lemma (2.1.10).

Theorem 2.2.2. Consider a closed subspace $M \subset H$. Then,

$$H = M \oplus M^\perp.$$

In other words, every $u \in H$ admits a unique decomposition $u = v + w$, where $v \in M$ and $w \in M^\perp$.

Corollary 2.2.3. Consider a subspace $M \subset H$. Then M is dense in H if and only if $M^\perp = \{0\}$.

Proof. Let $T = \overline{M}$. We want to prove that $T = H$. Using Theorem 2.2.2, it suffices to check that $T^\perp = \{0\}$. Since the inner product is continuous, then $T^\perp = M^\perp = \{0\}$.

On the other hand, since by definition T is closed, by Theorem 2.2.2 we have that $H = T \oplus T^\perp = T \oplus \{0\} = T$ as we wished. \square

A surprising property in Hilbert spaces is the fact that every linear and continuous function $T : H \rightarrow \mathbb{F}$ can be *represented* by some unique element in H . In what follows we assume that $\mathbb{F} = \mathbb{R}$.

Theorem 2.2.4 (Riesz Representation Theorem). *Let $T : H \rightarrow \mathbb{R}$ be a linear and continuous functional. Then, there exists a unique $u \in H$ such that*

$$Tv = (u, v), \quad \forall v \in H.$$

Moreover, let H^* be the dual space of H , that is, the space of all linear and continuous function from H to \mathbb{R} . Then the map $H^* \mapsto H$ is an isometric isomorphism (which we denote by \cong) where

$$\|u\|_H = \|T\|_{H^*}.$$

Remark 2.2.5. Notice how the inner product in Hilbert spaces has replaced the duality pairing defined for Banach spaces. In fact, in a certain sense, Riesz Representation Theorem (2.2.4) allows us to make a stronger statement regarding the dual spaces of Hilbert spaces and work in a more natural framework without ever resorting to the Hahn-Banach Theorem (2.1.3). For example, it is interesting to observe that the definition of orthogonality and orthogonal subspaces in Hilbert spaces (via the inner product) and Banach spaces (via the duality pairing) are essentially the same, with the distinction being an isomorphism between the Hilbert space and its dual. However, in certain cases, working with the definition of orthogonality in Banach spaces can be more useful as it allows for better generalization, such as when proving the density of a closed subspace.

A more general and useful result in our work is the Lax-Milgram Theorem.

Definition 2.2.6. We say that a bilinear form $a : H \times H \rightarrow \mathbb{R}$ is continuous and coercive if

- $|a(u, v)| \leq C\|u\| \|v\|, \quad \forall u, v \in H$
- $a(u, u) \geq \alpha\|u\|^2, \quad \forall u \in H$

respectively.

Theorem 2.2.7 (Lax-Milgram Theorem). *Let $a(u, v)$ be a bilinear, continuous and coercive bilinear form on H . If T is a linear and continuous functional in H , then there exists a unique $u \in H$ such that*

$$a(u, v) = T(v), \quad \forall v \in H.$$

In this section the well-known *Spectral Theorem* and the *Fredholm Alternative* are presented. With this in mind, we will now present key results and concepts (without proofs) that will provide the necessary foundation for stating the theorems.

Definition 2.2.8. A sequence $(e_n)_{n \in \mathbb{N}} \in H$ is a Hilbert basis of H if

1. $(e_n, e_m) = \begin{cases} 1, & n = m \\ 0, & n \neq m \end{cases}$;
2. $\overline{\text{span}\{(e_n)_{n \in \mathbb{N}}\}} = H$.

In a sense, a Hilbert basis resembles a basis in a finite-dimensional vector space.

Proposition 2.2.9. Let $(e_n)_{n \in \mathbb{N}}$ be a Hilbert basis of H . Then, for every $u \in H$, we can write

$$u = \sum_{k \in \mathbb{N}} (u, e_k) e_k \quad \text{and} \quad \|u\|^2 = \sum_{k \in \mathbb{N}} |(u, e_k)|^2.$$

The last equality is known as Parseval's identity.

The proposition above is particularly interesting because it allows us to express every element of H in terms of a countable basis. The following result guarantees the existence of a Hilbert basis if certain conditions are met.

Definition 2.2.10. We say that H is a separable Hilbert space if there exists a countable subset $M \subset H$ such that $\overline{M} = H$.

Theorem 2.2.11. Every separable Hilbert space admits an orthonormal Hilbert basis.

We now present some properties that our operators must satisfy in order to state the Spectral Theorem.

Definition 2.2.12. Consider a linear operator $T : H_1 \rightarrow H_2$, where H_1 and H_2 are Hilbert spaces.

1. Assume that $H = H_1 = H_2$ and $T \in \mathcal{L}(H)$. We say that T^* is the **adjoint** of T if

$$(y, Tx) = (T^*y, x), \quad \forall x, y \in H;$$

If $T = T^*$, i.e, if T and T^* domains (and their image) coincide we say that T is **self-adjoint**.¹

2. As above, let $T \in \mathcal{L}(H)$. We say that λ is an **eigenvalue** of T if $N(T - \lambda I) \neq \{0\}$. In that case we say that $\lambda \in \sigma(T)$ where $\sigma(T)$ is called the **spectrum** of T .² We also say that u is an **eigenvector** associated with the eigenvalue λ if $u \in N(T - \lambda I) \setminus \{0\}$.

¹The existence and uniqueness of T^* may not be obvious, but it follows from Riesz Representation Theorem (2.2.4). In any case, notice the similarities between this definition and the one given in Definition (2.1.1). In fact, in Banach spaces, the existence of the adjoint also comes from the Hahn-Banach Theorem (2.1.3)!

²Remarkably, in the infinite dimensional case, the set of eigenvalues $EV(T)$ may not coincide with the spectrum $\sigma(T)$. $T - \lambda I$ may fail to be invertible even if $T - \lambda I$ is injective.

We can derive some important properties regarding the spectrum of a compact operator and the spectrum of self-adjoint operators.

Proposition 2.2.13. *Let H be a Hilbert space and consider a compact operator $T \in \mathcal{L}(H)$. Then,*

- $0 \in \sigma(T)$;
- *one of the following holds:*
 - $\sigma(T) = \{0\}$;
 - $\sigma(T) \setminus \{0\}$ *is a finite set*;
 - $\sigma(T) \setminus \{0\}$ *is a sequence converging to 0*.

Proposition 2.2.14. *Let H be a Hilbert space and consider a self-adjoint operator $T \in \mathcal{L}(H)$. In this conditions, $\sigma(T)$ is real and eigenvectors corresponding to distinct eigenvalues are orthogonal.*

It is now possible to state on of the main results of this section.

Theorem 2.2.15 (Spectral Theorem for compact and self-adjoint operators). *Let H be a separable Hilbert space of infinite dimension and let $T \in \mathcal{L}(H)$ be a compact self-adjoint operator. Then, H admits a Hilbert basis $(e_n)_{n \in \mathbb{N}}$ such that*

$$Te_n = \lambda_n e_n$$

for $\lambda_n \in \mathbb{R}$, $\lambda_n \rightarrow 0$ as $n \rightarrow \infty$, where λ_n can be assumed to be a decreasing sequence.

2.3 Lebesgue and Sobolev Spaces

In this section, we apply the results and concepts from the previous ones. Besides the usual references already presented, we recommend [5], [6] and [7]. Let $\Omega \subset \mathbb{R}^d$ be an open set. Consider a *multi-index* $\alpha = (\alpha_1, \dots, \alpha_d) \in \mathbb{N}_0^d$, where $|\alpha| = \alpha_1 + \dots + \alpha_d$. Given a function defined in Ω , we denote its partial derivatives of order α by

$$D^\alpha = \frac{\partial^{|\alpha|}}{\partial x_1^{\alpha_1} \dots \partial x_d^{\alpha_d}}.$$

As usual, we denote the space of test functions with compact support in Ω by

$$\mathcal{D}(\Omega) = C_0^\infty(\Omega) = \{\varphi \in C^\infty(\Omega) : \text{supp } \varphi \text{ is compact in } \Omega\}.$$

Definition 2.3.1 (Lebesgue spaces). *Let $1 \leq p \leq \infty$. We define the Lebesgue space (L^p space)*

$$L^p(\Omega) = \left\{ u : \Omega \rightarrow \mathbb{R} : u \text{ is measurable and } \int_{\Omega} |f|^p < \infty \right\}$$

with the associated norm

$$\|f\|_{L^p(\Omega)} = \left(\int_{\Omega} |f|^p \right)^{\frac{1}{p}}.$$

If $p = \infty$ we set

$$L^\infty(\Omega) = \left\{ u : \Omega \rightarrow \mathbb{R} : u \text{ is measurable and } \exists C > 0 : |f(x)| \leq C \text{ a.e on } \Omega \right\}$$

with the associated norm

$$\|f\|_{L^\infty(\Omega)} = \inf \{ C : |f(x)| \leq C \text{ a.e on } \Omega \}$$

Definition 2.3.2. We say that $f \in L^1_{loc}(\Omega)$ if f is integrable in every compact $K \subset \Omega$, i.e.

$$f\chi_K \in L^1(\Omega), \quad \forall K \subset \Omega \text{ compact.}$$

This definition can be extended accordingly to every $L^p(\Omega)$ space, with $1 \leq p \leq \infty$.

Before introducing the notion of weak derivative in Sobolev spaces, it will be useful to dive into some Distribution theory. Consider the space of test functions $\mathcal{D}(\Omega)$ above. While we are not interested to define a topology in this space, we want to define linear and continuous functionals acting on $\mathcal{D}(\Omega)$. For now, it suffices to define (sequential) convergence in $\mathcal{D}(\Omega)$.

Definition 2.3.3. Let $(\varphi_n)_n \in \mathcal{D}(\Omega)$ and $\varphi \in \mathcal{D}(\Omega)$. If

1. $\forall n \in \mathbb{N}$ there exists a compact $K \subseteq \Omega$ such $\text{supp } \varphi_k \subseteq K$;
2. $\forall \alpha \in \mathbb{N}_0^d \quad \lim_n \|D^\alpha \varphi_n - D^\alpha \varphi\|_{L^\infty(\Omega)} = 0$

then we say that φ_n converges to φ in $\mathcal{D}(\Omega)$.

Definition 2.3.4 (Space of distributions). The dual space of $\mathcal{D}(\Omega)$, denoted by $\mathcal{D}^*(\Omega)$, is called the space of distributions, and we say that $T \in \mathcal{D}^*$ is a distribution.

A very illustrative example, with consequences when defining the duality pairing in Sobolev spaces, is that any locally integrable function $u \in L^1_{loc}(\Omega)$ defines a distribution. In fact, it is easy to prove that the operator T_u defined by

$$\begin{aligned} T_u : \mathcal{D}(\Omega) &\rightarrow \mathbb{R} \\ \varphi &\mapsto \int_{\Omega} u \varphi \end{aligned}$$

is linear and continuous. Therefore, one can give meaning to the action of a distribution over a test function, whenever the distribution is induced by a locally integrable function u . In this case, we can

write

$$\langle u, \varphi \rangle_{D^*(\Omega), D(\Omega)} = \int_{\Omega} u \varphi$$

where the duality pairing $\langle \cdot, \cdot \rangle_{D^*(\Omega), D(\Omega)}$ can be seen as a generalization of the $L^2(\Omega)$ inner product.

Definition 2.3.5 (Sobolev Spaces). *For $k \in \mathbb{N}$ and $1 \leq p \leq \infty$ we define the Sobolev space*

$$W^{k,p}(\Omega) = \{u \in L^p(\Omega) : D^\alpha u \in L^p(\Omega), \forall \alpha \in \mathbb{N}_0^d : |\alpha| \leq k\}$$

with the associated norms

- $1 \leq p < \infty$,

$$\|u\|_{W^{k,p}(\Omega)} := \left(\sum_{|\alpha| \leq k} \|D^\alpha u\|_{L^p(\Omega)}^p \right)^{\frac{1}{p}};$$

- $p = \infty$,

$$\|u\|_{W^{k,p}(\Omega)} := \max_{|\alpha| \leq k} \|D^\alpha u\|_{L^\infty(\Omega)}.$$

We say that $D^\alpha u$ is the weak derivative of order α of $u \in L^p(\Omega)$ if $D^\alpha u \in L^p(\Omega)$. The operator D^α is well-defined as a distribution, and satisfies

$$\int_{\Omega} D^\alpha u \varphi = (-1)^{|\alpha|} \int_{\Omega} u D^\alpha \varphi, \quad \forall \varphi \in \mathcal{D}(\Omega).$$

Throughout this work we are mostly concerned with Sobolev spaces with $p = 2$. In this case, we set $H^k(\Omega) := W^{k,2}(\Omega)$ which is a Hilbert space for the inner product³

$$(u, v) := \sum_{|\alpha| \leq k} (D^\alpha u, D^\alpha v)_{L^2(\Omega)}.$$

One of the main tools used in the last section of this chapter is the following embedding theorem that relates the topologies of $H^1(\Omega)$ and $L^2(\Omega)$.

Theorem 2.3.6 (Rellich Theorem). *Assume that Ω is a bounded Lipschitz domain. Then, the embedding $H^1(\Omega) \rightarrow L^2(\Omega)$ is compact, i.e., given the bounded sequence $(u_n)_{n \in \mathbb{N}} \subset H^1(\Omega)$ there exists a convergent subsequence $(u_{n_k})_{k \in \mathbb{N}} \subset L^2(\Omega)$.*

While we have only defined Sobolev spaces for $k \in \mathbb{N}$, it is possible to define fractional Sobolev spaces with a real exponent $s \in \mathbb{R}_0^+$. In particular, such a generalization can be made using Fourier Transforms if $p = 2$. Below we give an equivalent definition for a function $u \in H^k(\mathbb{R}^d)$.

³Observe that if $k = 0$ then $H^0(\Omega) = L^2(\Omega)$

Lemma 2.3.7. *Let $u \in L^2(\mathbb{R}^d)$. Then*

$$u \in H^k(\mathbb{R}^d) \iff (1 + |\xi|^k) \hat{u} \in L^2(\mathbb{R}^d)$$

where $\hat{u} = \mathcal{F}u$ denotes the Fourier Transform of u , given by $\mathcal{F}u(\xi) = \hat{u}(\xi) = \int_{\mathbb{R}^d} e^{-2\pi x\xi} u(x) d\xi$.

The above characterization of the $H^k(\mathbb{R}^d)$ space motivate the following definition

Definition 2.3.8. *Let $s \in \mathbb{R}$. We define*

$$H^s(\mathbb{R}^d) = \{u \in L^2(\mathbb{R}^d) : (1 + |\xi|^2)^{\frac{s}{2}} \hat{u} \in L^2(\mathbb{R}^d)\}$$

with the norm

$$\|u\|_{H^s(\mathbb{R}^d)} = \|(1 + |\xi|^2)^{\frac{s}{2}} \hat{u}\|_{L^2(\mathbb{R}^d)}.$$

The definition above only holds for Sobolev spaces defined over the whole space \mathbb{R}^d . In this work we are mostly concerned with the behavior over a bounded set $\Omega \subset \mathbb{R}^d$. Unfortunately, there are multiple definitions of fractional Sobolev spaces over a bounded set that may not agree between themselves if the boundary of Ω is not smooth enough (if the boundary fails to be parameterized by a continuous function). In any case, the following definition suffices for this work, see [8], [9] or [10].

Definition 2.3.9. *Let $\Omega \subset \mathbb{R}^d$ be a bounded set with Lipschitz boundary. We define*

$$\mathring{H}^s(\Omega) = \{v \in H^s(\mathbb{R}^d) : \text{supp } v \subset \overline{\Omega}\}$$

and

$$H^s(\Omega) = H^s(\mathbb{R}^d) \setminus \mathring{H}^s(\mathbb{R}^d \setminus \Omega).$$

The norm of a function $u \in H^s(\Omega)$ is given by

$$\|u\|_{H^s(\Omega)} = \inf\{\|\tilde{u}\|_{H^s(\mathbb{R}^d)} : \tilde{u} \in H^s(\mathbb{R}^d), \tilde{u}|_{\Omega} = u\}.$$

Fractional Sobolev spaces are important for our study because they are deeply related with the boundary behavior of a given function. For example, if $u \in H^1(\Omega)$ and Ω is bounded and a Lipschitz domain, then $u|_{\partial\Omega} \in H^{\frac{1}{2}}(\partial\Omega)$. However, the statement above must be defined rigorously: not only u is only defined in the open set Ω , but u is only defined *almost everywhere* and the Lebesgue measure of $\partial\Omega$ is zero. Intuitively, we consider the continuous extension of functions from Ω to the boundary $\partial\Omega$ which is only possible if domain is regular *enough*. This is done in context of trace theory, c.f [11] and [12].

Theorem 2.3.10. *Let Ω be a bounded set with Lipschitz boundary. Then, there exists a linear and continuous mapping called the trace operator*

$$\gamma_0 : H^1(\Omega) \rightarrow H^{\frac{1}{2}}(\partial\Omega)$$

that admits a bounded right inverse represented by γ_0^{-1} .

In particular, if $u \in H^2(\Omega)$, then $\frac{\partial u}{\partial x_j} \in H^1(\Omega)$ for $j = 1, \dots, d$ and the operator

$$\begin{aligned} \gamma_1 : H^2(\Omega) &\rightarrow L^2(\partial\Omega) \\ u &\mapsto \frac{\partial u}{\partial n} = \gamma_0(\nabla u) \cdot n \end{aligned}$$

is linear and continuous⁴.

The result above is stated in a very weak form since we are working in Lipschitz domains. If Ω is a smooth domain, then $\gamma_1 : H^2(\Omega) \rightarrow H^{\frac{1}{2}}(\partial\Omega)$ (c.f [5]). However, it should be noted that the normal derivative operator γ_1 cannot be defined if we only assume that $u \in H^1(\Omega)$. If such a continuous operator \mathcal{N} existed, then $\mathcal{N}\varphi = 0$ for every $\varphi \in \mathcal{D}(\Omega)$. By continuity, this would imply $\mathcal{N}u = 0$ for all $u \in H^1(\Omega)$, leading to a contradiction.

An important (closed) subspace of $H^1(\Omega)$ is the kernel of the trace operator γ_0 ,

$$\ker \gamma_0 = \{u \in H^1(\Omega) : \gamma_0 u = 0\} =: H_0^1(\Omega)$$

which can be equivalently defined as the closure of $\overline{\mathcal{D}(\Omega)}$ in the $H^1(\Omega)$ norm, i.e, $H_0^1(\Omega) := \overline{\mathcal{D}(\Omega)}^{H^1(\Omega)}$. $H_0^1(\Omega)$ is of major importance in the Dirichlet Laplacian problem, since the functions in $H_0^1(\Omega)$ "vanish" on $\partial\Omega$. Next, we state an important result to be used when studying the spectrum of the Dirichlet Laplacian.

Theorem 2.3.11 (Poincaré inequality). *Let Ω be a bounded set. Define $W_0^{1,p}(\Omega) := \overline{\mathcal{D}(\Omega)}^{W^{1,p}(\Omega)}$. Then, there exists $C > 0$ such that*

$$\|u\|_{L^p(\Omega)} \leq C \|\nabla u\|_{L^p(\Omega)}, \quad \forall u \in W_0^{1,p}(\Omega).$$

Finally, we shed some light over the dual space of Sobolev spaces (with fractional exponent). When working over the whole space \mathbb{R}^d one can prove the following result, c.f [13] or [14].

Theorem 2.3.12. *Let $s \in \mathbb{R}$ and $u \in H^s(\mathbb{R}^d)$. Then, any linear and continuous functional $T \in (H^s(\mathbb{R}^d))^*$ that acts in $H^s(\mathbb{R}^d)$ can be uniquely represented by some $v \in H^{-s}(\mathbb{R}^d)$ and the duality pairing is given*

⁴We take γ_0 as an element wise operator, where $\gamma_0(\nabla u) = \left(\gamma_0\left(\frac{\partial u}{\partial x_1}\right), \dots, \gamma_0\left(\frac{\partial u}{\partial x_d}\right)\right)$.

by

$$\langle T, u \rangle_{(H^s(\mathbb{R}^d))^*, H^s(\mathbb{R}^d)} = \int_{\mathbb{R}^d} \hat{u} \hat{v} = \int_{\mathbb{R}^d} (1 + |\xi|^2)^{\frac{s}{2}} \hat{u} (1 + |\xi|^2)^{-\frac{s}{2}} \hat{v} \leq \|u\|_{H^s(\Omega)} \|v\|_{H^{-s}(\Omega)}$$

where \hat{u} and \hat{v} represents the Fourier Transform of u and v , respectively. In particular, the dual of $H^s(\mathbb{R}^d)$ is isomorphic to $H^{-s}(\mathbb{R}^d)$.

Remark 2.3.13. Considering the inclusion $\mathcal{D}(\Omega) \subset H^s(\Omega)$, it is straightforward to observe that $(H^s(\Omega))^* \subset D^*(\Omega)$ which implies that $L^2(\Omega) \subset (H^s(\Omega))^* \cong H^{-s}(\Omega)$. Consequently, based on the preceding theorem, we note that Sobolev spaces with negative exponent s can be regarded as spaces of distributions with the following inclusions:

$$H^s(\Omega) \subset L^2(\Omega) \subset H^{-s}(\Omega)$$

In this case, one can consider $L^2(\Omega)$ as a pivot space, and by virtue of the identification of $L^2(\Omega)$ with its dual, the duality pairing $\langle \cdot, \cdot \rangle_{H^{-s}(\Omega), H^s(\Omega)}$ and the $L^2(\Omega)$ inner product coincide for every $u \in H^s(\Omega)$ and

$$\langle v, u \rangle_{H^{-s}(\Omega), H^s(\Omega)} = \int_{\Omega} uv$$

whenever it makes sense, i.e, when $v \in L^2(\Omega)$.

Theorem 2.3.10 allows to give some meaning to space $H^{-\frac{1}{2}}(\Omega)$. Let $u \in H^2(\Omega)$ and $v \in H^{\frac{1}{2}}(\partial\Omega)$. Then, $\gamma_0^{-1}v \in H^1(\Omega)$ and using Green's formula (see in the section below)

$$\langle \gamma_1 u, v \rangle_{H^{-\frac{1}{2}}(\partial\Omega), H^{\frac{1}{2}}(\partial\Omega)} = \int_{\Omega} \Delta u \gamma_0^{-1}v + \int_{\Omega} \nabla u \cdot \nabla \gamma_0^{-1}v$$

we have $\gamma_1 u \in H^{-\frac{1}{2}}(\Omega)$.

2.4 Spectral Decomposition of the Laplace Operator

In this section, we make a brief study regarding the Laplace Operator $-\Delta = -\sum_{n=1}^d \frac{\partial^2}{\partial x_n^2}$ in a bounded domain $\Omega \subset \mathbb{R}^d$ with Lipschitz boundary. Firstly, we recall the Divergence Theorem, e.g [15].

Theorem 2.4.1 (Divergence Theorem). *Let $\Omega \subset \mathbb{R}^d$ defined as above. Then,*

$$\int_{\Omega} \operatorname{div} \phi dx = \int_{\partial\Omega} \phi \cdot \mathbf{n} d\sigma,$$

where \mathbf{n} denotes the exterior unitary normal.

A main consequence of the Divergence Theorem are the well-known *Green's Formulas*, with major importance in this work.

Corollary 2.4.2 (Green's Formulas). *In this same conditions of the Theorem 2.4, let $u, v \in H^2(U)$. Then,*

1. $\int_{\Omega} \Delta u dx = \int_{\partial\Omega} \frac{\partial u}{\partial n} d\sigma;$
2. $\int_{\Omega} \Delta uv dx = - \int_{\Omega} \nabla u \cdot \nabla v dx + \int_{\partial\Omega} \frac{\partial u}{\partial n} v d\sigma;$
3. $\int_{\Omega} \Delta uv - u \Delta v dx = \int_{\partial\Omega} \frac{\partial u}{\partial n} v - \frac{\partial v}{\partial n} u d\sigma.$

Consider the following partial differential equation with null Dirichlet boundary conditions (the Neumann case is analogous)

$$\begin{cases} -\Delta u(x) = \lambda u(x), & \text{in } \Omega \\ u = 0, & \text{on } \partial\Omega. \end{cases} \quad (2.1)$$

The following the result is classical and can be found in numerous textbooks, see [3] [4], [16] or [17].

Theorem 2.4.3. *There exists a Hilbert basis $(u_n)_{n \in \mathbb{N}}$ of $L^2(\Omega)$ consisting of eigenfunctions u_n of $-\Delta$, i.e, for each $n \in \mathbb{N}$ there exists a pair eigenvalue/eigenfunction (λ_n, u_n) such that*

$$-\Delta u_n = \lambda_n u_n$$

where the sequence of eigenvalues can be ordered in an increasing order and $\lambda_n \rightarrow \infty$, $n \rightarrow \infty$. In particular, define $E_n = \text{span}\{u_1, \dots, u_n\}$ and the Rayleigh Quotient

$$R(u) = \frac{\|\nabla u\|_{L^2(\Omega)}^2}{\|u\|_{L^2(\Omega)}^2}.$$

Then,

$$\lambda_n = \min_{\substack{u \in E_{n-1}^\perp \\ u \neq 0}} R(u) = \max_{\substack{u \in E_n \\ u \neq 0}} R(u).$$

Proof. For each $f \in L^2(\Omega)$, we consider the problem

$$\begin{cases} -\Delta u(x) = f, & \text{in } \Omega \\ u = 0, & \text{on } \partial\Omega \end{cases}$$

with the associated variational form

$$\int_{\Omega} \nabla u \cdot \nabla v = \int_{\Omega} f v, \quad \forall v \in H_0^1(\Omega).$$

Using Lax-Milgram Theorem 2.2.7, it is straightforward to prove that the variational form above admits a unique weak solution $u \in H_0^1(\Omega)$ and the operator

$$T : L^2(\Omega) \rightarrow L^2(\Omega)$$

$$f \mapsto u$$

is well-defined. To prove that T is a compact operator, we use Poincaré and Cauchy-Schwarz inequalities and notice that

$$\alpha \|u\|_{H^1(\Omega)}^2 \leq \int_{\Omega} |\nabla u|^2 = \int_{\Omega} f u \leq \|f\|_{L^2(\Omega)} \|u\|_{L^2(\Omega)} \leq \|f\|_{L^2(\Omega)} \|u\|_{H^1(\Omega)} \implies \|u\|_{H^1(\Omega)} \leq C \|f\|_{L^2(\Omega)}$$

where $\alpha, C > 0$. The above result can be written as

$$\|Tf\|_{H^1(\Omega)} \leq C \|f\|_{L^2(\Omega)}, \quad \forall f \in L^2(\Omega)$$

and by Theorem 2.3.6 T is a compact operator. To check that T is self-adjoint it suffices to consider the weak variational form of the null Dirichlet boundary problems

$$-\Delta u = f \quad -\Delta v = g$$

for $f, g \in L^2(\Omega)$ and apply Green's formulas. It is also easy to see that $(Tf, f)_{L^2(\Omega)} \geq 0, \forall f \in L^2(\Omega)$ since

$$\int_{\Omega} (Tf)f = \int_{\Omega} u f = \|\nabla u\|_{L^2(\Omega)}^2 \geq 0.$$

Applying the Spectral Theorem 2.2.15 to T , there exists a Hilbert basis $(u_n)_{n \in \mathbb{N}}$ such that

$$Tu_n = \mu_n u_n$$

for $\mu_n \in \mathbb{R}, \mu_n \rightarrow 0$ as $n \rightarrow \infty$. In particular, taking $f = \lambda_n u_n$, where $\lambda_n = \frac{1}{\mu_n}$, one can write

$$-\Delta u_n = \lambda_n u_n,$$

or in the integral form

$$\int_{\Omega} |\nabla u|^2 = \lambda_n \int_{\Omega} u^2,$$

with $\lambda_1 \leq \lambda_2 \leq \dots \rightarrow \infty$. To check the variational form of the eigenvalues λ_n , let $u \in E_{n-1}^\perp$. Then,

$$\begin{aligned}
\|\nabla u\|_{L^2(\Omega)}^2 &= (\nabla u, \nabla u)_{L^2(\Omega)} = \left(\sum_{m \geq n} (u, u_m)_{L^2(\Omega)} \nabla u_m, \nabla u \right)_{L^2(\Omega)} \\
&= \sum_{m \geq n} (u, u_m)_{L^2(\Omega)} (\nabla u_m, \nabla u)_{L^2(\Omega)} \\
&= \sum_{m \geq n} \lambda_m (u, u_m)_{L^2(\Omega)} (u_m, u)_{L^2(\Omega)} \\
&\geq \lambda_n \sum_{m \geq n} |(u, u_m)_{L^2(\Omega)}|^2 \\
&= \lambda_n \|u\|_{L^2(\Omega)}^2
\end{aligned}$$

where we used the bilinearity of the inner product, the fact that the sequence λ_n is non-decreasing and the Parseval's identity. It is easy to check that the equality is only attained if and only if u is in the eigenspace of λ_k . This proves that

$$\lambda_n = \min_{\substack{u \in E_{n-1}^\perp \\ u \neq 0}} R(u).$$

The other case is analogous. □

3

From Spectral Theory to Geometry and Shape Optimization

Contents

3.1 The Laplace Operator	22
3.2 The Dirac Operator	25
3.3 A domain decomposition problem	31

Until otherwise indicated, let $\Omega \subset \mathbb{R}^d$ be an open and bounded domain with C^2 boundary, with $d \geq 2$.

We start by introducing the definition of a fundamental solution of a differential operator:

Definition 3.0.1. Consider the polynomial $p(\partial) = \sum_{i=0}^d c_i \frac{\partial}{\partial x_i}$, $c_i \in \mathbb{R}$ for each i . We say that the distribution $\Phi \in \mathcal{D}'(\mathbb{R}^n)$ is the fundamental solution of the partial differential operator $p(\partial)$ if

$$p(\partial)\Phi = \delta,$$

where δ is the Dirac Delta.

In particular, given Φ in the above conditions we have that $p(\partial)\Phi(x) = 0$, for $x \in \mathbb{R}^d \setminus \{0\}$. An important result in this context is Malgrange-Ehrenpreis theorem:

Theorem 3.0.2 (Malgrange-Ehrenpreis). Every constant partial differential operator $p(\partial)$, has a fundamental solution $\Phi \in \mathcal{D}'(\mathbb{R}^d)$.

Proof. See [18]. □

Below we present the fundamental solution of Laplace differential operator and some major results concerning Laplace and Helmholtz equations.

3.1 The Laplace Operator

In the following, we are going to study the Laplace operator ($-\Delta$ where $\Delta = \sum_{i=0}^d \frac{\partial^2}{\partial x_i^2}$) associated with the well-known Laplace equation

$$-\Delta u = 0. \tag{3.1}$$

Throughout this first part we are mostly concerned about its spectrum which is associated with the Helmholtz equation

$$-(\Delta + \lambda)u = 0 \iff -\Delta u = \lambda u \tag{3.2}$$

when subject to Dirichlet, Neumann or Robin boundary conditions.

By Theorem 3.0.2 we know that both equations (3.1) and (3.2) admit a fundamental solution that are given below.

Proposition 3.1.1. The function $\Phi : \mathbb{R}^d \setminus \{0\} \rightarrow \mathbb{R}$ given by

$$\Phi(x) = \begin{cases} -\frac{1}{2\pi} \log |x|, & d = 2 \\ \frac{1}{(n-2)|\partial B_1|} \frac{1}{|x|^{d-2}}, & d > 2 \end{cases}$$

is the fundamental solution of equation (3.1), where $|\partial B_1|$ denotes the boundary measure of the unitary ball.

Proposition 3.1.2. The function $\Phi_k : \mathbb{R}^d \setminus \{0\} \rightarrow \mathbb{R}$ given by

$$\Phi_k(x) = \begin{cases} \frac{i}{4} H_0^{(1)}(\sqrt{\lambda} \|x\|), & d = 2 \\ \frac{e^{i\sqrt{\lambda}\|x\|}}{4\pi\|x\|}, & d > 2 \end{cases}$$

is the fundamental solution of equation (3.2), where $H_0^{(1)}$ is the Hankel function of first kind and order 0.

Remark 3.1.3. We note that the fundamental solutions presented above are not unique. Given the linearity of the Laplace operator, if $\Phi(x)$ is a fundamental solution of Equation 3.1 then, $\Phi(x) + v(x)$ is also a fundamental solution of Laplace equation assuming that $v(x)$ is harmonic. However, we choose the fundamental solutions above since they present a radial behavior which is important to the numerical method to be presented in Chapter 4

Definition 3.1.4. We say that $\lambda \in \mathbb{C}$ is an eigenvalue of equation (3.2) if there exists an eigenfunction function $u \not\equiv 0 \in C^2(\Omega) \cap C(\overline{\Omega})$ such that

$$\begin{cases} -\Delta u(x) = \lambda u(x), & x \in \Omega \\ u(x) = 0, & x \in \partial\Omega \end{cases}$$

Remark 3.1.5. We note that, in some literature, it is common to write Equation 3.2 as $-\Delta u = \kappa^2 u$, where κ is known as an eigenfrequency and $\kappa^2 = \lambda$. This is a consequence of the fact that Equation 3.2 can be derived from the wave Equation where we also use some constant in the form c^2 , $c \in \mathbb{R}$. As such, if using eigenfrequencies, the fundamental solution in Proposition 3.1.2 would change accordingly the consideration above.

Some shape optimization results

In this chapter we present some important results regarding shape optimization. More precisely, we're interested in problems of the form

$$\min\{F(\lambda_1(\Omega), \dots, \lambda_k(\Omega)) : |\Omega| = c\}, \quad (3.3)$$

where F is a function of the first k eigenvalues of the Helmholtz equation (3.2) and $c > 0$.

Theorem 3.1.6 (Faber-Krahn inequality). The ball of volume c minimizes the first eigenvalue λ_1 of (3.2)

over all open and bounded domains $\Omega \subset \mathbb{R}^d$, that is

$$\min\{\lambda_1(\Omega) : |\Omega| = c\}.$$

In particular, it can be shown that

$$\lambda_1 \geq \frac{\pi j_{\frac{d}{2}-1,1}^2}{c}$$

where $j_{n,k}$ is the k -th zero of the Bessel function J_n .

Theorem 3.1.6 is a classic form of an isoperimetric inequality, conjectured for the first time by Lord Rayleigh. More recently, a reverse of the Faber-Krahn inequality was proven in [19],

Theorem 3.1.7. *Let Ω be a bounded convex domain of \mathbb{R}^d and denote the inradius of Ω (radius of the largest ball contained within the domain) by ρ_Ω . Then,*

$$\lambda(\Omega) \leq \frac{|\partial\Omega|}{d\rho_\Omega|\Omega|} \lambda(\mathbb{D})$$

While Faber-Krahn inequality deals with the first eigenvalue of the Helmholtz equation, other results have been uncovered for the second and third eigenvalues:

Theorem 3.1.8 (Krahn-Szegő). *The domain that minimizes the quantity*

$$\min\{\lambda_2(\Omega) : |\Omega| = c\}$$

consists of two equal and disjoint balls of volume $\frac{c}{2}$.

Theorem 3.1.9 (Bucur-Henrot). *There exists a domain Ω that minimizes the quantity*

$$\min\{\lambda_3(\Omega) : |\Omega| = c\}.$$

More recently, Bucur (see [20]) was able to assert the existence of, at least, one solution to problem (3.3). More specifically we can state the following theorem:

Theorem 3.1.10 (Bucur). *For every $k \in \mathbb{N}$ problem*

$$\min\{\lambda_k(\Omega) : |\Omega| = c\}$$

as at least one solution. Moreover, every solution is bounded and has finite perimeter.

In this work we are also interested in the study of the eigenvalues of polygonal domains like triangles and quadrilaterals. An important property of these domains is the fact that they allow for the so-called

Steiner symmetrization which preserves the area of these polygons while decreasing the perimeter and the first eigenvalue. This type of transformation allow us to state the following result:

Theorem 3.1.11 (Pólya-Szegő). *The quantity $\lambda_1|\Omega|$ is minimized for equilateral triangles among every triangle where the inequality*

$$\frac{4\pi^2}{\sqrt{3}} \leq \lambda_1(T)$$

holds for every triangle T of area 1. Analogously, $\lambda_1|\Omega|$ is minimized for the square among every quadrilateral.

Related to triangles, we can also cite the recent work of Serrano and Orriols ([21]) based on a previous work of Antunes and Freitas ([22]) conjectured that the three first eigenvalues define the shape of a triangle (such result resembles a lot the famous Marc Kac question ([23]) if one can "hear the shape of a drum", that is, if given the frequencies produced by a drum one could identify the drum's shape, which has proven to be false (see [24])). In any case, Serano and Orriols were able to show that not any three eigenvalues suffice to fully characterize the shape of a triangle:

Theorem 3.1.12 (Serrano-Orriols). *There exist two triangles T_A and T_B not isometric to each other such that $\lambda_i(T_A) = \lambda_i(T_B)$, for $i = 1, 2, 4$.*

Other important results in this area are related with the ratio and gap between the first eigenvalues.

Theorem 3.1.13 (Ashbaugh-Benguria). *The solution of the maximization problem*

$$\max \left\{ \frac{\lambda_2(\Omega)}{\lambda_1(\Omega)} : |\Omega| < \infty \right\}$$

is the ball. In particular, it can be shown that

$$\frac{\lambda_2(\Omega)}{\lambda_1(\Omega)} \leq \frac{j_{\frac{n}{2},1}^2}{j_{\frac{n}{2}-1,1}^2}.$$

Remark 3.1.14. *Note that in theorem above we do not make any constraint regarding the volume of our domain (except finite measure). This easily follows from the variational form given in Theorem ?? and the fact that we are now considering a ratio between two eigenvalues in the same domain.*

3.2 The Dirac Operator

Motivated by recent advancements in nuclear, molecular physics and the discovery of very interesting electrical, mechanical and thermal properties, Dirac materials have resurged a lot of attention in the Dirac equation. Discovered by Paul Dirac in 1928 ([25]), Dirac equation was able to successfully merge the

famous Schrödinger equation with special relativity, while explaining the weird phenomena that today is known as *spin*. Capable of describe the relativistic dynamics of spin- $\frac{1}{2}$ particles (like the electron), one can determine the energy states by studying the spectrum of the Hamiltonian (Dirac) operator \hat{H} in $L^2(\Omega, \mathbb{C}^2)$

$$\hat{H}u = Eu \quad \text{with} \quad \hat{H} = c \mathbf{a} \cdot \mathbf{p} + mc^2 \beta + V(x) \mathbb{I}_4,^1 \quad (3.4)$$

where $\mathbf{p} = -i\nabla$ is the momentum operator, c is the speed of light, m is the electron mass, E is the electron energy, $V(x)$ is the vector potential and $u \in L^2(\Omega, \mathbb{C}^2)$ is a four-spinor. One of the major problems regarding the study of Dirac's equation is the fact that, unlike Schrödinger equation, it has a matrix structure that is given by Pauli matrices

$$\sigma_x = \begin{bmatrix} 0 & 1 \\ 1 & 0 \end{bmatrix} \quad \sigma_y = \begin{bmatrix} 0 & -i \\ i & 0 \end{bmatrix} \quad \sigma_z = \begin{bmatrix} 1 & 0 \\ 0 & -1 \end{bmatrix}$$

which can be found incorporated in the 4×4 matrices \mathbf{a} and β :

$$a_i = \begin{bmatrix} 0 & \sigma_i \\ \sigma_i & 0 \end{bmatrix} \quad \beta = \begin{bmatrix} \mathbb{I}_2 & 0 \\ 0 & \mathbb{I}_2 \end{bmatrix}.$$

Setting the potential $V(x) = 0$ and considering $\Omega \subset \mathbb{R}^2$ be a bounded and open domain with C^3 boundary, we can rewrite equation (3.4) in the form

$$\begin{bmatrix} m & -i(\partial_1 - i\partial_2) \\ -i(\partial_1 + i\partial_2) & m \end{bmatrix} \begin{bmatrix} u_1(x) \\ u_2(x) \end{bmatrix} = E \begin{bmatrix} u_1(x) \\ u_2(x) \end{bmatrix} \quad (3.5)$$

where we let $u(x) = \begin{bmatrix} u_1(x) \\ u_2(x) \end{bmatrix}$. In particular, we are interested in studying the so-called *infinite-mass boundary conditions* which are implemented through the operator domain

$$D(\hat{H}) = \{u \in H^1(\Omega, \mathbb{C}^2) : u_2 = i(n_1 + in_2)u_1 \text{ on } \Omega\}.$$

For a point $x \in \partial\Omega$, we denote by $n(x) = (n_1(x), n_2(x))^T$ the outward unit vector to Ω and $\tau(x) = (n_2(x), -n_1(x))^T$ the unit tangent such that $(\tau(x), n(x))$ is a positively-oriented orthonormal basis of \mathbb{R}^2 . Considering the arc-length parametrization of $\partial\Omega$ given by the map

$$s : [0, L) \rightarrow \mathbb{R}^2, \quad s(t) = \int_0^t \|r'(\sigma)\| d\sigma$$

where L represents the arc-length of $\partial\Omega$ and r is a parametrization of $\partial\Omega$, we denote by $\kappa : \partial\Omega \rightarrow \mathbb{R}$ the signed curvature of $\partial\Omega$ where the *Frenet-Serret* formula (we dropped the dependency of s in the

¹ In the following, we will be using natural units, with $c = 1$.

parameter t)

$$\frac{\partial \tau}{\partial s} = \kappa(s)n(s)$$

holds. Just like the Helmholtz operator above, we start by stating some major properties regarding Dirac Operator.

Proposition 3.2.1. *The eigenvalues and eigenfunctions of equation (3.5) have the following properties:*

- *The eigenvalues are real and the spectrum of the Dirac operator is discrete. Also, the spectrum is symmetric with respect to zero and the eigenvalues can be arranged as follows*

$$-\infty \leftarrow \dots \leq -\lambda_3 \leq -\lambda_2 \leq -\lambda_1 < 0 < \lambda_1 \leq \lambda_2 \leq \lambda_3 \leq \dots \rightarrow \infty;$$

- *The principal (first) eigenvalue can be described using the variational form*

$$\lambda_1^2 = \min_{0 \neq u \in D(\hat{H})} \frac{\|\nabla u\|_2^2 + m^2 \|u\|_2^2 + m \|\gamma u\|_2^2}{\|u\|_2^2}$$

where $\gamma : H^1(\Omega, \mathbb{C}^2) \rightarrow L^2(\partial\Omega, \mathbb{C}^2)$ denotes the trace of u .

- *Assuming $m = 0$ and $\Omega = \mathbb{D}$, we have that the first eigenvalue is the solution to the equation*

$$J_0(\lambda) = J_1(\lambda)$$

and the associated eigenfunction is (in polar coordinates)

$$u(r, \theta) = \begin{pmatrix} J_0(\lambda r) \\ ie^{i\theta} J_1(\lambda r) \end{pmatrix}.$$

For future comparison, the numerical approximation of λ is $\lambda \approx 1.434696$.

The following proposition regarding the lack of separable solutions of the Dirac operator will have important consequences in the numerical approach to solve Dirac equation. However, we start by stating and proving the following auxiliary lemma:

Lemma 3.2.2. *Let $u \in H^2(\Omega)$ a solution of (3.5) and $u \in D(\hat{H})$. Then we have*

$$\|\hat{H}u\|_{L^2(\Omega)}^2 = \|\nabla u\|_{L^2(\Omega)}^2 + m^2 \|u\|_{L^2(\Omega)}^2 + m \|\gamma u\|_{L^2(\partial\Omega)}^2 - \frac{1}{2} \int_{\partial\Omega} \kappa |u|^2 d\sigma \quad (3.6)$$

Proof. Recalling the $L^2(\Omega)$ inner product for complex functions

$$(f, g)_{L^2(\partial\Omega)} = \int_{\Omega} f \bar{g} dx,$$

(3.6) can be rewritten as

$$\|\hat{H}u\|_{L^2(\Omega)}^2 = m^2\|u_1\|_{L^2(\Omega)}^2 + m^2\|u_2\|_{L^2(\Omega)}^2 \quad (3.7)$$

$$+ im \int_{\Omega} u_1(\partial_1 + i\partial_2)\bar{u}_2 dx - im \int_{\Omega} \bar{u}_1(\partial_1 - i\partial_2)u_2 dx \quad (3.8)$$

$$+ im \int_{\Omega} \bar{u}_2(\partial_1 + i\partial_2)u_1 dx - im \int_{\Omega} u_2(\partial_1 - i\partial_2)\bar{u}_1 dx \quad (3.9)$$

$$+ \|(\partial_1 - i\partial_2)u_2\|_{L^2(\Omega)}^2 + \|(\partial_1 + i\partial_2)u_1\|_{L^2(\Omega)}^2. \quad (3.10)$$

We now address each line of the expression above individually:

- For (3.7) we directly have

$$m^2\|u\|_{L^2(\Omega)}^2.$$

- For (3.8) we integrate by parts the first part:

$$\int_{\Omega} u_1(\partial_1 + i\partial_2)\bar{u}_2 dx = \int_{\partial\Omega} u_1\bar{u}_2(1+i)d\sigma - \int_{\Omega} \bar{u}_2(\partial_1 + i\partial_2)u_1 dx$$

where the last part cancels with the first part of (3.9).

- Analogously, for (3.9) we obtain a similar result for the last part

$$\int_{\Omega} u_2(\partial_1 - i\partial_2)\bar{u}_1 dx = \int_{\partial\Omega} u_2\bar{u}_1(1-i)d\sigma - \int_{\Omega} \bar{u}_1(\partial_1 - i\partial_2)u_2 dx$$

where the last part cancels with the last part of (3.8).

- For (3.10) we firstly deduced the following property:

$$\operatorname{Im} \left(\int_{\Omega} \partial_1 v \partial_2 \bar{v} dx \right) = \frac{1}{2i} \int_{\partial\Omega} \bar{v} \partial_{\tau} v d\sigma, \quad \forall v \in H^2(\Omega),$$

where $\partial_{\tau} v = \tau \cdot \nabla v$, which can be obtained using integration by parts. Then, for each part we have

$$\begin{aligned} \|(\partial_1 - i\partial_2)u_2\|_{L^2(\Omega)}^2 &= \|\nabla u_2\|_{L^2(\Omega)}^2 + i \left(\int_{\Omega} \partial_1 u_2 \partial_2 \bar{u}_2 dx - \int_{\Omega} \partial_2 u_2 \partial_1 \bar{u}_2 dx \right) \\ &= \|\nabla u_2\|_{L^2(\Omega)}^2 + i \int_{\partial\Omega} \bar{u}_2 \partial_{\tau} u_2 d\sigma \end{aligned}$$

$$\begin{aligned} \|(\partial_1 + i\partial_2)u_1\|_{L^2(\Omega)}^2 &= \|\nabla u_1\|_{L^2(\Omega)}^2 - i \left(\int_{\Omega} \partial_1 u_1 \partial_2 \bar{u}_1 dx - \int_{\Omega} \partial_2 u_1 \partial_1 \bar{u}_1 dx \right) \\ &= \|\nabla u_1\|_{L^2(\Omega)}^2 - i \int_{\partial\Omega} \bar{u}_1 \partial_{\tau} u_1 d\sigma \end{aligned}$$

where we used the property above.

As such, we can write everything as

$$\begin{aligned}\|\hat{H}u\|_{L^2(\Omega)}^2 &= m^2\|u\|_{L^2(\Omega)}^2 + im\left(\int_{\partial\Omega} u_1\bar{u}_2(1+i)d\sigma - \int_{\partial\Omega} u_2\bar{u}_1(1-i)d\sigma\right) \\ &\quad + \|\nabla u\|_{L^2(\Omega)}^2 + i\left(\int_{\partial\Omega} \bar{u}_2\partial_\tau u_2 d\sigma - \int_{\partial\Omega} \bar{u}_1\partial_\tau u_1 d\sigma\right).\end{aligned}$$

Finally, using the boundary conditions $u_2 = i(n_1 + in_2)u_1$, we conclude that

$$im\left(\int_{\partial\Omega} u_1\bar{u}_2(1+i)d\sigma - \int_{\partial\Omega} u_2\bar{u}_1(1-i)d\sigma\right) = \|\gamma u\|_{L^2(\partial\Omega)}^2$$

while

$$i\int_{\partial\Omega} \bar{u}_2\partial_\tau u_2 d\sigma - i\int_{\partial\Omega} \bar{u}_1\partial_\tau u_1 d\sigma = -\frac{1}{2}\int_{\partial\Omega} \kappa|u|^2 d\sigma$$

where we used the Frenet-Serret formula above and the fact that at $\partial\Omega$ we have $|u_1|^2 = |u_2|^2$. \square

Proposition 3.2.3. *Let $u \in H^2(\Omega)$ a solution of (3.5) and $u \in D(\hat{H})$. Then u cannot be written using separable solutions.*

Proof. We start by showing that $|\lambda| > m$ for any eigenvalue λ if $\kappa = 0$ a.e. Assuming that there exists an eigenvalue λ associated with an eigenfunction u such that $|\lambda| \leq m$, by using Lemma 3.2.2 we get that

$$\|\nabla u\|_{L^2(\Omega)}^2 + m\|\gamma u\|_{L^2(\partial\Omega)}^2 \leq 0 \implies \|\nabla u\|_{L^2(\Omega)} = 0 \wedge m\|\gamma u\|_{L^2(\partial\Omega)} = 0$$

and u must be a constant, which does not satisfy the boundary conditions.

Since $u \in H^2(\Omega)$, using (3.5), we can express u_2 as

$$u_2 = \frac{-i(\partial_1 + i\partial_2)u_1}{\lambda + m}$$

allowing us to rewrite Dirac equation (3.5) using the Helmholtz equation with Cauchy–Riemann oblique boundary conditions:

$$\begin{cases} -\Delta u_1 = (\lambda^2 - m^2)u_1, & \text{in } \Omega \\ i(\partial_1 + i\partial_2)u_1 + (\lambda + m)i(n_1 + in_2)u_1 = 0, & \text{on } \Omega. \end{cases} \quad (3.11)$$

The rest of the proof will have in consideration two domain types: triangular (on a wedge) and rectangular.

1. Consider Ω to be a wedge domain with angle θ (see Figure 4.1):

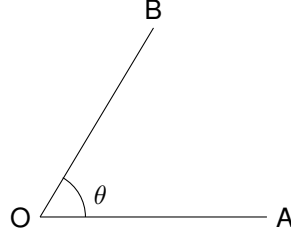


Figure 3.1: A wedge domain with an interior angle θ .

In this case, since the outward unit normal on \overline{OA} is $n = \begin{pmatrix} 0 \\ -1 \end{pmatrix}$ and on \overline{OB} is $n = \begin{pmatrix} -\sin \theta \\ \cos \theta \end{pmatrix}$, using polar coordinates system (3.11) transforms into

$$\begin{cases} \left(\partial_r^2 + \frac{1}{r} \partial_r + \frac{1}{r^2} \partial_\theta^2 \right) u_1 = (\lambda^2 - m^2) u_1, & \text{in } \Omega \\ i(\cos \theta \partial_r - \frac{1}{r} \sin \theta \partial_\theta + i(\sin \theta \partial_r + \frac{1}{r} \cos \theta \partial_\theta)) u_1 + (\lambda + m) u_1 = 0, & \text{on } \overline{OA} \\ i(\cos \theta \partial_r - \frac{1}{r} \sin \theta \partial_\theta + i(\sin \theta \partial_r + \frac{1}{r} \cos \theta \partial_\theta)) u_1 + (\lambda + m) i(-\sin \theta + i \cos \theta) u_1 = 0, & \text{on } \overline{OB} \end{cases} \quad (3.12)$$

As such, assuming that exists a solution $u_1(r, \theta) = \phi(r)T(\theta)$ of the system (3.12), from the boundary condition of \overline{OB} one finds the equation

$$\frac{e^{i\theta} (\phi(r)T'(\theta) + rT(\theta) ((\lambda + m)\phi(r) - i\phi'(r)))}{r} = 0$$

which can be rewritten as

$$\frac{T(\theta)}{T'(\theta)} = -\frac{\phi(r)}{r(m\phi(r) + \lambda\phi(r) - i\phi'(r))} = -k^2$$

for some $k \in \mathbb{R}$. Solving the equations above we find that

$$u_1(r, \theta) = A e^{-\frac{\theta}{k^2}} r^{\frac{i}{k^2}} e^{-ir(\lambda+m)}, \quad A \in \mathbb{R} \setminus \{0\}.$$

Substituting in the boundary condition for \overline{OA} we obtain

$$A(1 + e^{i\theta}) r^{\frac{i}{k^2}} (\lambda + m) e^{-\frac{\theta}{k^2} - ir(\lambda+m)} = 0$$

where we conclude that $\lambda = -m$ (since if $\theta = \pi$ we would have a degenerate wedge), a contradiction.

2. For rectangular domains, we point the proof in [26].

□

Remark 3.2.4. A careful reader will note that two important details are being overlooked: triangular domains or quadrilaterals do not have the required smoothness to obtain the formula (3.6) (and signed curvature is not defined everywhere, only on each edge where $\kappa = 0$), neither u has enough regularity to be integrated by parts while expanding (3.10). We point to [27], where such details can be found for triangles, but are analogous for quadrilaterals.

We now present some open conjectures that we try numerically address in this work:

Conjecture 3.2.5 (A Faber-Krahn type inequality). *Let $m \geq 0$ and $\Omega \subset \mathbb{R}^2$ an open and Lipschitz domain. Then,*

$$\lambda_1(\Omega) \geq \lambda_1(\Omega^*)$$

where Ω^* is the disk of the same area or perimeter as Ω .

Conjecture above is regarded as a hot open problem in spectral geometry [28]. In [29] a geometric lower bound for the first (non-negative) eigenvalue was found, while in [30] a sharp upper bound (a reverse Faber-Krahn type inequality, like in Theorem 3.1.7) was proved to hold for convex domains with C^3 boundary. However, due to the difficulty of the problem, simpler versions with domain restrictions to triangles and rectangles are being studied. For example, in [26] a study for rectangles was conducted, where the conjectures below were proved under some extra hypothesis:

Conjecture 3.2.6 (Shape optimization in rectangles). *Given $m \geq 0$, let $\lambda_1(a, b) = \lambda_1(\Omega_{a,b})$ denote the first eigenvalue of the Dirac Operator with infinite-mass boundary conditions in a rectangle with sides a and b . Then,*

1. *Area constraint:* $\lambda_1(a, \frac{1}{a}) \geq \lambda_1(1, 1), \forall a > 0;$
2. *Perimeter constraint:* $\lambda_1(a, 2 - a) \geq \lambda_1(1, 1), \forall a \in (0, 2).$

In the same vain, in [27] very similar results were proven for triangles:

Conjecture 3.2.7 (Shape optimization in triangles). *Consider the triangle $\Omega_{a,b}$ defined by the points $O = (0, 0), A = (a, 0), B = (0, b)$ for $a, b > 0$. Then, given any $m \geq 0$,*

1. *Area constraint:* $\lambda_1(a, b) \geq \lambda(k, k), \forall a, b, k > 0$ such that $ab = k^2;$
2. *Perimeter constraint:* $\lambda_1(a, b) \geq \lambda(k, k), \forall a \in (0, (2 + \sqrt{2})k)$ and $\forall b, k > 0$ such that $a + b + \sqrt{a^2 + b^2} = (2 + \sqrt{2})k.$

3.3 A domain decomposition problem

We now consider the polygonal domain $\Omega \subset \mathbb{R}^2$ which we divide into two non-overlapping regions Ω_1 and Ω_2 such that $\overline{\Omega} = \overline{\Omega_1} \cup \overline{\Omega_2}$. We denote their common boundary by $\gamma = \partial\Omega_1 \cap \partial\Omega_2$ and denote by

$\Gamma_i = \partial\Omega_1 \setminus \gamma$ the boundary of each domain Ω_i minus the common boundary. The problem we address this section is to find functions u_1, u_2 such that

$$\begin{aligned} -\nabla k_i \nabla u_i &= f_i, \text{ in } \Omega_i \\ u_1 - u_2 &= 0, \text{ on } \gamma \\ k_1 \frac{\partial u_1}{\partial n_1} + k_2 \frac{\partial u_2}{\partial n_2} &= 0, \text{ on } \gamma \\ u_i &= 0, \text{ on } \Gamma_i \end{aligned} \quad (3.13)$$

where $k_1 \geq k_2 > 0$ are constants, $f_i \in L^2(\Omega_i)$ is a source function on each domain and n_i is the (normalized) outward normal to each domain subdomain $\Omega_i, i = 1, 2$. Finally, we will write $n = n_1 = -n_2$ when we are restricted to the interface.

In what follows we mainly used the reference [31]. Equations (3.13) can be used to study a system of two bodies with different material parameters (contact resistance or thermal conductivity) connected by an interface γ . If we set

$$f = \begin{cases} \frac{f_1}{k_1}, & \Omega_1 \\ \frac{f_2}{k_2}, & \Omega_2 \end{cases},$$

then the problem above can be seen as a natural reformulation of the Poisson equation

$$\begin{aligned} -\Delta u &= f, \text{ in } \Omega \\ u &= 0, \text{ on } \partial\Omega \end{aligned} \quad (3.14)$$

where f is (possibly) discontinuous on the interface γ . In order to keep the equivalence between both problems, we enforce some transmission conditions in Equations (3.13) using the continuity of the solutions and the continuity of their normal derivative on γ . To establish the equivalence between both problems we write the variational weak form associated with them. For (3.14) it's an easy process: we multiply the equation in Ω by a test function $v \in C_0^\infty(\Omega)$ and using Green's Identity we find that

$$a(u, v) = \int_{\Omega} \nabla u \cdot \nabla v = \int_{\Omega} f v$$

where a is the associated bilinear form. As such, enlarging our functional space to the Hilbert Space $V^0 = H_0^1(\Omega)$, our problem can be rewritten as

$$\text{find } u \in V^0 : a(u, v) = (f, v), \forall v \in V^0 \quad (3.15)$$

which has a unique solution in V^0 by virtue of Lax-Milgram lemma. In fact, by regularity results (see Section 6.3.1 of [7]), we're looking for $u \in V^0 \cap H_{\text{loc}}^2(\Omega')$, $\forall \Omega' \Subset \Omega^2$.

For (3.13) the process is not so direct. For the first equation, for the subdomain Ω_1 , we multiply it

²We say that $A \Subset B$ when \bar{A} is compact and $\bar{A} \subset B$.

with a test function in $v_1 \in C_0^\infty(\Omega_1)$ and integrate by parts where we get

$$a(u_1, v_1) = \int_{\Omega_1} \nabla u_1 \cdot \nabla v_1 = \left(\frac{f_1}{k_1}, v_1 \right)$$

and analogously, for the subdomain Ω_2 , considering $v_2 \in C_0^\infty(\Omega_2)$ we find

$$a(u_2, v_2) = \int_{\Omega_2} \nabla u_2 \cdot \nabla v_2 = \left(\frac{f_2}{k_2}, v_2 \right).$$

To add the interface condition on the normal derivative we notice that if we take $v \in C_0^\infty(\Omega)$, we can define $v_1 = v|_{\Omega_1}$ and $v_2 = v|_{\Omega_2}$, where $v_i \in C^\infty(\Omega_i)$ and $v_i(x) = 0$, $\forall x \in \Gamma_i$ for $i = 1, 2$. This allows us to write that

$$\begin{aligned} - \int_{\Omega_1} k_1 \Delta u_1 v_1 - \int_{\Omega_2} k_2 \Delta u_2 v_2 &= \int_{\Omega_1} k_1 \nabla u_1 \cdot \nabla v_1 + \int_{\Omega_2} k_2 \nabla u_2 \cdot \nabla v_2 \\ &\quad - k_1 \int_{\gamma} \frac{\partial u_1}{\partial n_1} v_1 - k_2 \int_{\gamma} \frac{\partial u_2}{\partial n_2} v_2 \end{aligned}$$

We observe that if $v_{1|\gamma} = v_{2|\gamma} = \eta$, then using the condition on the normal derivative we would find that

$$\int_{\Omega_1} k_1 \nabla u_1 \cdot \nabla v_1 + \int_{\Omega_2} k_2 \nabla u_2 \cdot \nabla v_2 = (f_1, v_1) + (f_2, v_2).$$

As such, we consider the continuous extension operator P_i from the interface to each domain Ω_i such that $(P_i \eta)|_{\gamma} = \eta$. In that case, given a function μ defined in γ^3 , the identity above holds if we rewrite it in the form

$$\int_{\Omega_1} k_1 \nabla u_1 \cdot \nabla P_1 \mu + \int_{\Omega_2} k_2 \nabla u_2 \cdot \nabla P_2 \mu = (f_1, P_1 \mu) + (f_2, P_2 \mu).$$

Finally, for the continuity on the interface we just enforce that $u_1 = u_2$ on γ . The process above allow us to state the weak form of problem (3.13) in the result below.

Proposition 3.3.1. *Consider the set of equations (3.13) and the bilinear form $a_i = (w_i, v_i) = (\nabla w_i, \nabla v_i)$.*

Let

$$\begin{aligned} V_i &= \{v_i \in H^1(\Omega_i) : v_{i|\partial\Omega \cap \partial\Omega_i} = 0\}; \\ V_i^0 &= H_0^1(\Omega_i) \\ \Lambda &= \{\eta \in H^{\frac{1}{2}}(\gamma) : \eta = v|_{\gamma} \text{ for some } v \in V^0\} \end{aligned}$$

³A description of such function will be given below, when we formalize the weak form of the problem. For now assume that such extension has the regularity that we need.

where $V^0 = H_0^1(\Omega)$ as above. Then the weak formulation of (3.13) reads as

$$\text{find } u_1 \in V_1, u_2 \in V_2 \text{ such that } \begin{cases} a_1(u_1, v_1) = (\frac{f_1}{k_1}, v_1), \forall v_1 \in V_1^0 \\ a_2(u_2, v_2) = (\frac{f_2}{k_2}, v_2), \forall v_2 \in V_2^0 \\ u_1 = u_2, \text{ on } \gamma \\ a_1(k_1 u_1, P_1 \mu) + a_2(k_2 u_2, P_2 \mu) = (f_1, P_1 \mu) + (f_2, P_2 \mu), \forall \mu \in \Lambda \end{cases} \quad (3.16)$$

where the operator $P_i : \Lambda \rightarrow V_i$ is continuous for $i = 1, 2$.

Remark 3.3.2. The existence of the (continuous) extension operators P_1 and P_2 is not obvious. See [32] or [5] for the existence of such operator.

We are now ready to prove the equivalence between both problems:

Theorem 3.3.3. Problem (3.15) is equivalent to (3.16).

Proof. (\implies) :

Let $u \in V^0$ be a solution of problem (3.15). We start by defining $u_1 = u_{\Omega_1}$ and $u_2 = u_{\Omega_2}$. It's clear that u_1 and u_2 satisfy equations 1 and 2 of (3.16).

For equation 3, we use the fact that $u \in H^1(\Omega)$ and therefore $u \in H_{\text{loc}}^2(\Omega)$. Given Ω' such that $\Omega' \Subset \Omega$ and $\gamma \subset \Omega'$, we have that $u \in H^2(\Omega')$ and $u \in C^{0,\lambda}(\overline{\Omega'})$ (u is in the Hölder Space of exponent λ ; see Theorem 4.12 of [32] for more details.) As such, u is continuous on the interface and $u_1 = u_2$ on γ .

Finally, given $\mu \in \Lambda$, we can define the function

$$P\mu = \begin{cases} P_1 \mu \\ P_2 \mu \end{cases}$$

which satisfies $P\mu \in V^0$ and the equality 4 in (3.16).

(\impliedby) :

Let $u_1 \in V_1^0, u_2 \in V_2^0$ be the two solutions of problem (3.15). We now set

$$u = \begin{cases} u_1, & \text{in } \Omega_1 \\ u_2, & \text{in } \Omega_2 \end{cases}.$$

In this case, we again notice that for $i = 1, 2$ we have $u_i \in H_{\text{loc}}^2$ which implies that u_1 and u_2 is Hölder continuous and therefore u is also Hölder continuous since $u_1 = u_2$ on the interface, by assumption. Therefore, we also have that $u \in V^0$.

Defining $P\mu$ like above, we take $\mu \in \Lambda$ for some $v \in V$ such that $\mu = v|_\gamma$. As such, we have that the difference $(v|_{\Omega_i} - P_i\mu) \in V_i^0$ for each $i = 1, 2$ and

$$\begin{aligned} a(ku, v) &= \left[a_1(k_1u_1, v|_{\Omega_1} - P_1\mu) + a_1(k_1u_1, P_1\mu) \right] + \left[a_2(k_2u_2, v|_{\Omega_2} - P_2\mu) + a_2(k_2u_2, P_2\mu) \right] \\ &= \left[(f_1, v|_{\Omega_1} - P_1\mu) + (f_1, P_1\mu) \right] + \left[(f_2, v|_{\Omega_2} - P_2\mu) + (f_2, P_2\mu) \right] \\ &= (\tilde{f}, v), \implies a(u, v) = (f, v) \end{aligned}$$

where we take $\tilde{f} = \begin{cases} f_1, & \text{in } \Omega_1 \\ f_2, & \text{in } \Omega_2 \end{cases}$ as an auxiliary function and used the assumptions 1, 2 and 4 of equations (3.16). \square

Remark 3.3.4. *The above result is important because, as we will see, the Method of Fundamental Solutions only addresses the solution of each subdomain Ω_i independently (for which we have density and convergence results for functions in H^1) while enforcing the interface conditions. By the result above we're, in fact, in the conditions of our numerical method since each function belongs to a closed subspace of $H^1(\Omega_i)$ for $i = 1, 2$.*

Posteriori estimate:

We now look to prove that the error obtained in the numerical approximation using the MFS only depends on the boundary and interface error. With that in mind, we start by introducing some auxiliary results and concepts that we need. See [33], [7] or [6].

Lemma 3.3.5. *Let $\Omega \subset \mathbb{R}^d$ be a smooth, bounded domain and $u \in C^2(\overline{\Omega})$. Then, for every $x \in \Omega$,*

$$u(x) = - \int_{\Omega} \Phi(x-y) \Delta u(y) dy + \int_{\partial\Omega} \Phi(x-y) \frac{\partial u}{\partial n}(y) - u(y) \frac{\partial \Phi}{\partial n}(x-y) d\sigma(y)$$

Proof. See Theorem 3.11 in [34].⁴ \square

Lemma 3.3.6. *Consider $u \in C^2(\overline{\Omega})$ in the same conditions as in Lemma 3.3.5. Assume that there exists $\varphi(x, \cdot) \in C^2(\overline{\Omega})$ such that*

$$\begin{cases} \Delta_y \varphi = 0, & y \in \Omega \\ \varphi(x, y) = \Phi(x-y), & y \in \partial\Omega \end{cases}$$

for every $x \in \Omega$. Then

$$\int_{\partial\Omega} \Phi(x-y) \frac{\partial u}{\partial n}(y) d\sigma(y) = \int_{\Omega} \varphi(x, y) \Delta u(y) dy + \int_{\partial\Omega} \frac{\partial \varphi}{\partial n_y}(x, y) u(y) d\sigma(y).$$

⁴The proof given in the reference assumes weaker assumptions than the ones listed here. This lemma can be proven just assuming that $u \in C^2(\Omega) \cap C^1(\overline{\Omega})$, Ω is a *normal* domain (like rectangles), and we are in the conditions of the Divergence Theorem.

Proof. Using Green's third identity we find that

$$\begin{aligned} \int_{\Omega} \underbrace{\Delta_y \varphi(x, y) u(y) - \varphi(x, y) \Delta u(y)}_{=0} dy &= \int_{\partial\Omega} \frac{\partial \varphi}{\partial n_y}(x, y) u(y) - \varphi(x, y) \frac{\partial u}{\partial n}(y) d\sigma(y) \\ &= \int_{\partial\Omega} \frac{\partial \Phi}{\partial n_y}(x - y) u(y) - \Phi(x - y) \frac{\partial u}{\partial n}(y) d\sigma(y) \end{aligned}$$

as we wanted. \square

Definition 3.3.7 (Green's function). *With the same assumptions as in Lemma 3.3.6, we define the Green's function of Ω as*

$$G(x, y) = \Phi(x - y) - \phi(x, y), \quad \forall x \in \Omega, y \in \bar{\Omega}, x \neq y$$

which satisfies

$$\begin{cases} \Delta_y G(x, y) = \delta_x, & y \in \Omega \\ G(x, y) = 0, & y \in \partial\Omega \end{cases}.$$

We say that the fundamental solution $\Phi(x - y)$ is the singular part of G and $\varphi(x, y)$ is the regular part.

Remark 3.3.8. *The existence of the Green function for a general domain Ω depends on the solvability of the problem*

$$\begin{cases} \Delta_y \varphi = 0, & y \in \Omega \\ \varphi(x, y) = \Phi(x - y), & y \in \partial\Omega \end{cases}$$

which can be asserted for a Lipschitz domain. See Theorem 3.8 in [33]⁵.

Assuming that the domain admits a Green function, then we can improve on Lemma 3.3.5. Given $u \in C^2(\Omega) \cap C^1(\bar{\Omega})$ we can represent it as

$$u(x) = \int_{\Omega} G(x, y) \Delta u(y) dy - \int_{\partial\Omega} \frac{\partial G}{\partial n_y}(x, y) u(y) d\sigma(y).$$

In particular, if u satisfies the Poisson equation with Dirichlet boundary conditions, then

$$u(x) = \int_{\Omega} G(x, y) f(y) dy - \int_{\partial\Omega} \frac{\partial G}{\partial n_y}(x, y) g(y) d\sigma(y).$$

⁵Observe that $\forall y \in \partial\Omega$, $\phi(x, y) = \Phi(x - y)$ is never singular since $x \in \Omega$

Lemma 3.3.9. *Let Ω be a smooth, open and bounded set. Then $\forall x \in \Omega, y \in \partial\Omega$*

$$\begin{aligned}\frac{\partial G}{\partial n_y}(x, y) &< 0 \\ \frac{\partial \Phi}{\partial n_y}(x - y) &< 0.\end{aligned}$$

Proof. Let $u \in C^2(\Omega) \cap C^1(\bar{\Omega})$ be a solution of

$$\begin{cases} \Delta u(x) = 0, x \in \Omega \\ u(x) = g(x), x \in \partial\Omega \end{cases}$$

where g is a nonnegative and arbitrary continuous function (it is known that such u exists). By the maximum principle (applied to $-u$) we know that $u(x) > 0$. Since u can be represented by

$$u(x) = - \int_{\partial\Omega} \frac{\partial G}{\partial n_y}(x, y) g(y) \sigma(y)$$

we find that the integral above is negative, which implies that $\frac{\partial G}{\partial n_y}(x, y)$ must also be negative because g is arbitrary. To prove that

$$\frac{\partial \Phi}{\partial n_y}(x - y) < 0$$

it suffices to notice that Φ is radially symmetric and $\Phi(x) = \Phi(r)$, with $r \in \mathbb{R}_0^+$ and $\Phi'(r) = -\frac{1}{2\pi r} < 0$. \square

Let $u = (u_1, u_2)$ be the solution of (3.13) and $\tilde{u} = (\tilde{u}_1, \tilde{u}_2)$ the numerical approximation given by the method of fundamental solutions. Then, we have that

$$\begin{cases} -\Delta u_i &= 0, \text{ in } \Omega_i \\ u_1 &= u_2, \text{ on } \gamma \\ \frac{\partial u_1}{\partial n} &= \frac{\partial u_2}{\partial n}, \text{ on } \gamma \\ u_i &= 0, \text{ on } \Gamma_i \end{cases} \quad \begin{cases} -\Delta \tilde{u}_i &= 0, \text{ in } \Omega_i \\ \tilde{u}_1 &= \tilde{u}_2 + \tilde{g}_1, \text{ on } \gamma \\ \frac{\partial \tilde{u}_1}{\partial n} &= \frac{\partial \tilde{u}_2}{\partial n} + \tilde{g}_2, \text{ on } \gamma \\ \tilde{u}_i &= \tilde{h}_i, \text{ on } \Gamma_i \end{cases} \quad (3.17)$$

where $\tilde{g}_i \in L^\infty(\gamma)$, $\tilde{h}_1 \in L^\infty(\Gamma_i)$ are the numerical approximation at γ and Γ_i (we recall that our numerical approximation satisfies (3.14) in the interior of each Ω_i by construction).

We now state and prove the desired *Posteriori* estimate.

Theorem 3.3.10. *Consider u and \tilde{u} defined as above and assume that Ω is a smooth and bounded domain of \mathbb{R}^2 . Then, there exists a constant $C > 0$ that only depends on the domains Ω_1 and Ω_2 such that*

$$\|u - \tilde{u}\| \leq C(\|\tilde{g}_1\| + \|\tilde{g}_2\| + \|\tilde{h}_1\| + \|\tilde{h}_2\|)$$

Proof. Using the representation Lemma 3.3.5 we find that

$$\begin{aligned} u_1(x) &= \int_{\Gamma_1} \Phi(x-y) \frac{\partial u_1}{\partial n_1}(y) d\sigma(y) + \int_{\gamma} \Phi(x-y) \frac{\partial u_1}{\partial n}(y) - u_1(y) \frac{\partial \Phi}{\partial n}(x-y) d\sigma(y) \\ u_2(x) &= \int_{\Gamma_2} \Phi(x-y) \frac{\partial u_2}{\partial n_2}(y) d\sigma(y) - \left(\int_{\gamma} \Phi(x-y) \frac{\partial u_2}{\partial n}(y) - u_2(y) \frac{\partial \Phi}{\partial n}(x-y) d\sigma(y) \right) \end{aligned}$$

where we used the fact that u_1 and u_2 vanish on the boundaries Γ_1 and Γ_2 , respectively, and $\frac{\partial u_2}{\partial n_2} = -\frac{\partial u_2}{\partial n}$ since $n = n_1 = n_2$ on the interface. Analogously, we can represent \tilde{u}_1 and \tilde{u}_2 in the integral form

$$\begin{aligned} \tilde{u}_1(x) &= \int_{\Gamma_1} \Phi(x-y) \frac{\partial \tilde{u}_1}{\partial n_1}(y) - \tilde{h}_1(y) \frac{\partial \Phi}{\partial n_1}(x-y) d\sigma(y) + \int_{\gamma} \Phi(x-y) \frac{\partial \tilde{u}_1}{\partial n}(y) - \tilde{u}_1(y) \frac{\partial \Phi}{\partial n}(x-y) d\sigma(y) \\ \tilde{u}_2(x) &= \int_{\Gamma_2} \Phi(x-y) \frac{\partial \tilde{u}_2}{\partial n_2}(y) - \tilde{h}_2(y) \frac{\partial \Phi}{\partial n_2}(x-y) d\sigma(y) - \left(\int_{\gamma} \Phi(x-y) \frac{\partial \tilde{u}_2}{\partial n}(y) - \tilde{u}_2(y) \frac{\partial \Phi}{\partial n}(x-y) d\sigma(y) \right) \end{aligned}$$

$$\begin{aligned} (u_1 - \tilde{u}_1)(x) &= \int_{\Gamma_1} \Phi(x-y) \left(\frac{\partial u_1}{\partial n_1}(y) - \frac{\partial \tilde{u}_1}{\partial n_1}(y) \right) d\sigma(y) + \int_{\Gamma_1} \tilde{h}_1(y) \frac{\partial \Phi}{\partial n_1}(x-y) d\sigma(y) \\ &\quad + \int_{\gamma} \Phi(x-y) \left(\frac{\partial u_1}{\partial n}(y) - \frac{\partial \tilde{u}_1}{\partial n}(y) \right) - \left(u_1(y) - \tilde{u}_1(y) \right) \frac{\partial \Phi}{\partial n}(x-y) d\sigma(y) \end{aligned}$$

$$\begin{aligned} (u_2 - \tilde{u}_2)(x) &= \int_{\Gamma_2} \Phi(x-y) \left(\frac{\partial u_2}{\partial n_2}(y) - \frac{\partial \tilde{u}_2}{\partial n_2}(y) \right) d\sigma(y) + \int_{\Gamma_2} \tilde{h}_2(y) \frac{\partial \Phi}{\partial n_2}(x-y) d\sigma(y) \\ &\quad + \int_{\gamma} -\Phi(x-y) \left(\frac{\partial u_2}{\partial n}(y) - \frac{\partial \tilde{u}_2}{\partial n}(y) \right) + \left(u_2(y) - \tilde{u}_2(y) \right) \frac{\partial \Phi}{\partial n}(x-y) d\sigma(y) \end{aligned}$$

Since,

$$(u - \tilde{u})(x) = \chi_{\Omega_1}(u_1 - \tilde{u}_1)(x) + \chi_{\Omega_2}(u_2 - \tilde{u}_2)(x)$$

and writing

$$\tilde{h}(x) = \begin{cases} \tilde{h}_1(x), \Gamma_1 \\ \tilde{h}_2(x), \Gamma_2 \end{cases}$$

$$\begin{aligned} (u - \tilde{u})(x) &= \int_{\partial\Omega} \Phi(x-y) \left(\frac{\partial u}{\partial n}(y) - \frac{\partial \tilde{u}}{\partial n}(y) \right) d\sigma(y) + \int_{\partial\Omega} \tilde{h}(y) \frac{\partial \Phi}{\partial n}(x-y) d\sigma(y) \\ &\quad - \int_{\gamma} \Phi(x-y) \tilde{g}_2 - \tilde{g}_1 \frac{\partial \Phi}{\partial n}(x-y) d\sigma(y) \end{aligned}$$

□

4

The Method of Fundamental Solutions

Contents

4.1	Density and linear independence results	40
4.2	Numerical approach for the Laplace Equation	47
4.2.1	An enrichment technique	49
4.3	Numerical approach for the Helmholtz Equation	52
4.3.1	The Subspace Angle Technique	53

4.1 Density and linear independence results

The method of Fundamental Solutions is the base method to be implemented throughout this work. As a meshless method, it does not involve any kind of domain discretization (into some mesh) like in finite differences or finite elements methods. Instead, the problem is now of point placement. Since the mesh creation is one of the most computational expensive parts of the methods above, one of the main advantages of the MFS is exactly the lack of it.

As the name implies, MFS is based on the fundamental solutions of a previously known PDE. Consider the Elliptic linear differential operator \mathcal{L} with fundamental solution Φ such that $\mathcal{L}\Phi(x) = \delta, \forall x \in \mathbb{R}^d$. Intuitively, we can consider the approximation

$$\tilde{u}(x) = \sum_{j=1}^N \alpha_j \Phi(x - y_j)$$

to the partial differential equation with a linear boundary operator \mathcal{B}

$$\begin{cases} \mathcal{L}u(x) = 0, x \in \Omega \\ \mathcal{B}u(x) = 0, x \in \partial\Omega \end{cases}.$$

By definition and using the linearity of the operator \mathcal{L} , \tilde{u} satisfies the equation in Ω , and the coefficients α_j can be determined by imposing the boundary conditions

$$\mathcal{B}\tilde{u}(x) = \sum_{j=1}^N \alpha_j \mathcal{B}\Phi(x - y_j) = 0,$$

where $y_j \in \hat{\Gamma} \subset \mathbb{R}^d \setminus \overline{\Omega}$ with $j = 1, \dots, N$, are the so-called source points to be chosen. We chose them to be outside our domain since, by translation, the Fundamental Solution Φ has a singularity at each y_j because, otherwise, it would render our approximation full of singularities inside Ω .

Remark 4.1.1. While the motivation above might seem far-fetched, one can observe that the approximation \tilde{u} resembles a convolution between some density function $\alpha(x)$ and the fundamental solution Φ . As we will see below, it can be proven that the fundamental solutions of the operator \mathcal{L} are dense in the functional space defined in $\partial\Omega$ (which is enough since, as we already saw, the interior condition is satisfied by construction). In general, that allow us to approximate $u(x)$ using the single layer potential

$$\int_{\Gamma} \Phi(x - y) \varphi(y) d\sigma(y) \approx \sum_{j=1}^N w_j \varphi(y_j) \Phi(x - y_j) = \tilde{u}(x) \quad (4.1)$$

where $\varphi(y)$ is a layer density to be determined and $y_j \in \hat{\Gamma}$ and w_j are the nodes and weights of some quadrature, respectively. Setting $\alpha_j = w_j \varphi(y_j)$ we recover the approximation given above.

First, we introduce the notion of *artificial boundary* (or *pseudo-boundary*), which is analyzed in [35].

Definition 4.1.2. A source set $\hat{\Gamma}$ is said to be admissible if

1. $\hat{\Gamma} \subset \mathbb{R}^d \setminus \overline{\Omega}$ is an open set with components in each external part of Ω ;
2. $\hat{\Gamma} = \partial\hat{\Omega}$ is the boundary of $\hat{\Omega}$, where $\hat{\Omega} \subset \mathbb{R}^d \setminus \overline{\Omega}$ is an open set with components in each external part of Ω . Note that the problem must be well posed in $\hat{\Omega}$;
3. $\hat{\Gamma} \subset \partial\hat{\Omega}$, when $\partial\hat{\Omega}$ is an analytical boundary set verifying (2.) and $\hat{\Gamma}$ is open in the $\partial\hat{\Omega}$ topology.

We denote the set of chosen source points by $\mathcal{Y} = \{y_j \in \hat{\Gamma} : j = 1, \dots, N\}$.

Throughout this work, the adopted source set will always be the second option since it provides better numerical results. However, notice that the density results below still hold when considering different types of admissible source sets.

For now, assume that $\mathcal{L} = -\Delta$ and Φ is the fundamental solution of the Laplace equation. In the appropriate functional space and given an admissible source set $\hat{\Gamma}$, we consider the approximation space

$$\mathcal{S}(\Gamma, \hat{\Gamma}) = \text{span}\{\Phi(x - y)|_{x \in \Gamma} : y \in \hat{\Gamma}\}.$$

Some preliminary results are going to be needed in order to present the desired density proofs. We notice that every result below has its own counterpart if we consider $\mathcal{L} = -(\Delta + k^2)$ and Φ_k to be fundamental solution of the Helmholtz equation. We start by introducing the concept of analytic continuation. For further details see [36].

Definition 4.1.3. Let f be a complex valued function defined on $\Omega \subset \mathbb{C}$. We say that f is holomorphic on Ω if for every $a \in \Omega$, there exists a neighborhood U of a and $(c_n)_{n \in \mathbb{N}} \subset \mathbb{C}$ such that the power series

$$\sum_{n=0}^{\infty} c_n (z - a)^n$$

converges to $f(z)$ for every $z \in U$.

Theorem 4.1.4 (Analytic continuation). Let f be a holomorphic function in the connected subset $\Omega \subset \mathbb{C}$. If there exists a non-empty $U \subset \Omega$ such that $f = 0$ in U , then $f = 0$ in Ω .

As seen in the above remark, the study of layer potentials plays an important role in the Method of Fundamental Solutions, which are now formalized, and some results are stated. Since this by itself a large topic see [13], [37] and [38] for more details.

Definition 4.1.5. Let Ω be a bounded domain of class C^2 and $\varphi \in H^{\frac{1}{2}}(\Omega)$. The functions

$$S\varphi(x) = \int_{\partial\Omega} \Phi(x - y)\varphi(y)d\sigma(y)$$

and

$$M\varphi(x) = \int_{\partial\Omega} \frac{\partial\Phi(x-y)}{\partial n} \varphi(y) d\sigma(y)$$

are called the single and double layer potentials with density φ , respectively.

Proposition 4.1.6. *Let Ω be a bounded domain of class C^2 and $\varphi \in H^{\frac{1}{2}}(\Omega)$. Then the single layer potential is harmonic in $\mathbb{R}^d \setminus \overline{\partial\Omega}$, continuous across $\partial\Omega$, and for every $x \in \partial\Omega$ we have the following jump relations for the normal derivative:*

$$\lim_{z \rightarrow x} \frac{\partial S\varphi}{\partial n^-}(z) = \int_{\partial\Omega} \frac{\partial\Phi(x-y)}{\partial n} \varphi(y) d\sigma(y) - \frac{1}{2}\varphi(x), \quad z \in \mathbb{R}^d \setminus \overline{\Omega}$$

and

$$\lim_{z \rightarrow x} \frac{\partial S\varphi}{\partial n^+}(z) = \int_{\partial\Omega} \frac{\partial\Phi(x-y)}{\partial n} \varphi(y) d\sigma(y) + \frac{1}{2}\varphi(x), \quad z \in \Omega.$$

In particular, we have

$$\varphi(x) = \frac{\partial S\varphi}{\partial n^+}(x) - \frac{\partial S\varphi}{\partial n^-}(x), \quad \forall x \in \partial\Omega.$$

Analogously, the double layer potential is harmonic in $\mathbb{R}^d \setminus \overline{\partial\Omega}$, its normal derivative is continuous across $\partial\Omega$, and for every $x \in \partial\Omega$ we have the following jump relations:

$$\lim_{z \rightarrow x} M^+\varphi(z) = \int_{\partial\Omega} \frac{\partial\Phi(x-y)}{\partial n} \varphi(y) d\sigma(y) + \frac{1}{2}\varphi(x), \quad z \in \mathbb{R}^2 \setminus \overline{\Omega}$$

and

$$\lim_{z \rightarrow x} M^-\varphi(z) = \int_{\partial\Omega} \frac{\partial\Phi(x-y)}{\partial n} \varphi(y) d\sigma(y) - \frac{1}{2}\varphi(x), \quad z \in \Omega$$

In particular, we have

$$\varphi(x) = M^+\varphi(x) - M^-\varphi(x), \quad \forall x \in \partial\Omega.$$

Lastly, it will be useful to study the well-posedness of the exterior Dirichlet problem for the Laplace Equation, c.f [33].

Theorem 4.1.7 (Well-Posedness of the Exterior Dirichlet problem). *Let Ω be a bounded and open subset of \mathbb{R}^2 . Then, there exists a unique solution $u \in C^2(\Omega^c) \cap C(\overline{\Omega^c})$ of the exterior Dirichlet Laplacian problem given by*

$$\begin{cases} \Delta u = 0, & \text{in } \mathbb{R}^2 \setminus \overline{\Omega} \\ u = 0, & \text{on } \partial\Omega \\ u(x) = \mathcal{O}(1), & \text{for } |x| \rightarrow \infty. \end{cases}$$

Remark 4.1.8. Notice that the condition at infinity must be enforced to have uniqueness. Otherwise, one could easily find a family of solutions up to a multiplicative constant (if $u(x)$ is a solution, then $\alpha u(x)$

would also be a solution for any $\alpha \in \mathbb{R}$).

The main result which justifies the MFS for the Laplace equation is now stated. The proof given here is slightly different from the ones in [8], [35]. It is also influenced by the proofs in [39].

Theorem 4.1.9. *Let Ω be an open and bounded set with C^2 boundary $\Gamma = \partial\Omega$ such that $\overline{\Omega} \subset \hat{\Omega} \subset \mathbb{R}^2$, where $\hat{\Omega}$ is an open and bounded set and $\hat{\Gamma} = \partial\hat{\Omega}$ is an admissible source set. Then, $\mathcal{S}(\Gamma, \hat{\Gamma}) \oplus \mathbb{R}$ is dense in $H^{\frac{1}{2}}(\Gamma)$ and in $H^{-\frac{1}{2}}(\Gamma)$.*

Proof. In view of Lemma (2.1.10) we start by fixing some notation. Let $E = H^{\frac{1}{2}}(\Gamma)$. For every (fixed) $y \in \hat{\Gamma}$, the maps

$$\begin{aligned}\Phi(\cdot - y) : \varphi &\mapsto \int_{\Gamma} \Phi(x - y) \varphi(x) d\sigma(x) \\ 1 : \varphi &\mapsto \int_{\Gamma} \varphi(x) d\sigma(x)\end{aligned}$$

are linear and continuous in $H^{\frac{1}{2}}(\Gamma)$, and $1, \Phi(\cdot - y) \in H^{-\frac{1}{2}}(\Gamma)$ (notice that $1, \Phi(\cdot - y) \in L^1_{\text{loc}}(\mathbb{R}^2)$ and $1, \Phi(\cdot - y) \in L^2(\hat{\Gamma})$).

Observe that $\mathcal{S}(\Gamma, \hat{\Gamma}) \oplus \mathbb{R} = \text{span}\{1, \Phi\}$ and let $N = \text{span}\{1, \Phi\} \subset H^{-\frac{1}{2}}(\Gamma)$. Using the Definition (2.1.9),

$$N^{\perp} = \{\varphi \in H^{\frac{1}{2}}(\Gamma) : \langle \psi, \varphi \rangle = 0, \forall \psi \in N\}$$

our goal is to prove that $N^{\perp} = \{0\}$. Let $\varphi \in N^{\perp}$ and consider $w(y) = \int_{\Gamma} \Phi(x - y) \varphi(x) d\sigma(x)$, $y \in \mathbb{R}^2$. Then,

$$\int_{\Gamma} \Phi(x - y) \varphi(x) d\sigma(x) = 0, \forall y \in \hat{\Gamma} \quad (4.2)$$

and

$$\int_{\Gamma} \varphi(x) d\sigma(x) = 0. \quad (4.3)$$

In order to verify that $w(y)$ satisfies the exterior Laplace problem with Dirichlet boundary conditions, one can use the fact that w exhibits the asymptotic behavior

$$w(y) = -\frac{1}{2\pi} \int_{\Gamma} \varphi(x) d\sigma(x) \log |y| + \mathcal{O}(1), \quad |y| \rightarrow \infty$$

and condition (4.3), to check that w is bounded at infinity. Therefore, by condition (4.2)

$$\begin{cases} \Delta w = 0, & \text{in } \mathbb{R}^2 \setminus \hat{\Omega} \\ w(y) = 0, & \text{on } \hat{\Gamma} \\ w(y) = \mathcal{O}(1), & |y| \rightarrow \infty. \end{cases}$$

Since the problem above is well-posed, its unique solution is $w(y) = 0$, $\forall y \in \mathbb{R}^2 \setminus \overline{\hat{\Omega}}$. By (a unique) analytic continuation (see Theorem (4.1.4)), we can extend w by zero in $\mathbb{R}^2 \setminus \overline{\Omega}$. Since w is a single layer potential over Γ , w is continuous on Γ and therefore, by continuity, $w = 0$ on Γ . Once again, using the fact that the single layer potential is harmonic in Ω , w satisfies the (inner) Laplace problem

$$\begin{cases} \Delta w = 0, & \text{in } \Omega \\ w(y) = 0, & \text{on } \Gamma \end{cases}$$

which, by uniqueness, implies that $w = 0$ in $\hat{\Omega}$. Finally, we can conclude that $\varphi = 0$ in Γ by Proposition (4.1.6) since the normal derivate jump is zero.

Therefore, we can write $N^\perp = \{0\}$ and by Lemma (2.1.10)

$$\mathcal{S}(\Gamma, \hat{\Gamma}) \oplus \mathbb{R} = \overline{\text{span}\{1, \Phi\}} = \{0\}^\perp$$

given the fact that $H^{\frac{1}{2}}(\Omega)$ is reflexive. Since $0 \in H^{\frac{1}{2}}(\Gamma)$ (and $0 \in H^{-\frac{1}{2}}(\Gamma)$) then $\mathcal{S}(\Gamma, \hat{\Gamma}) \oplus \mathbb{R}$ is dense in $H^{\frac{1}{2}}(\Gamma)$ and in $H^{-\frac{1}{2}}(\Gamma)$ (this is to be expected since $H^s(\Omega)$ is dense in $H^{-s}(\Omega)$ for $s > 0$). \square

Finally, the discretization argument to be presented follows from the fact that, given a set of source points $\mathcal{Y} = \{y_1, \dots, y_N\} \subset \mathbb{R}^2 \setminus \overline{\Omega}$, the fundamental solutions $\Phi(\cdot - y_1), \dots, \Phi(\cdot - y_N)$ are linearly independent on $\partial\Omega$ and therefore in Ω .

Theorem 4.1.10. *Let \mathcal{Y} be a set of source points, as defined above. Then, the restriction of the functions $\Phi(\cdot - y_1), \dots, \Phi(\cdot - y_N)$ to $\partial\Omega$ are linearly independent.*

Proof. Assume that $\tilde{u}(x) = \sum_{j=1}^N \alpha_j \Phi(x - y_j) = 0$, $\forall x \in \partial\Omega$. We prove that $\alpha_1 = \dots = \alpha_N = 0$. Since, by construction, \tilde{u} satisfies the Laplace equation and by assumption $\tilde{u}(x) = 0$, $\forall x \in \partial\Omega$, by the well-posedness of the interior Dirichlet problem, $\tilde{u} = 0$ in $\overline{\Omega}$. Again, by analytic continuation, $\tilde{u} = 0$ in $\mathbb{R}^2 \setminus \mathcal{Y}$. Applying the Laplace operator to \tilde{u} , by linearity

$$\sum_{j=1}^N \alpha_j \delta y_j = 0$$

which implies that $\alpha_1 = \dots = \alpha_N = 0$ by the linear independence of the Dirac deltas. \square

Consider now the operator $\mathcal{L} = -(\Delta + k^2)$, and assume that k is **not** an eigenfrequency of the Helmholtz equation. Just like stated above, the results presented for the fundamental solution of the Laplace Equation still hold for the fundamental solution of the Helmholtz equation. However, a different type of infinity conditions must be considered, the so-called *Sommerfeld Radiation Conditions*, c.f [38].

Theorem 4.1.11 (Well-Posedness of the Exterior Dirichlet problem of the Helmholtz Equation). *Let Ω be a bounded and open subset of \mathbb{R}^2 . Then, there exists a unique solution $u \in C^2(\Omega^c) \cap C(\overline{\Omega^c})$ of the exterior Dirichlet Helmholtz problem given by*

$$\begin{cases} -\Delta u = k^2 u, & \text{in } \mathbb{R}^2 \setminus \overline{\Omega} \\ u = 0, & \text{on } \partial\Omega \\ |x| \left(\frac{x}{|x|} \nabla u(x) - ik \right) u(x) = 0, & \text{for } |x| \rightarrow \infty. \end{cases}$$

Remark 4.1.12. *Just like the exterior Dirichlet problem for the Laplace Equation, the Well-Posedness of the exterior Helmholtz Problem depends on the conditions at infinity. In this case, they are known as Sommerfeld Radiation Conditions and are of the form*

$$|x|^{\frac{d-1}{2}} \left(\frac{x}{|x|} \nabla u(x) - ik \right) u(x) = 0, \text{ for } |x| \rightarrow \infty,$$

where d stands for the space dimension. We also notice that the single layer potential given by

$$\int_{\Gamma} \Phi_k(x-y) \varphi(x) d\sigma(x)$$

satisfies the Sommerfeld Radiation Condition, when $|y| \rightarrow \infty$.

Analogously to the Laplace problem, consider the space

$$\mathcal{S}(\Gamma, \hat{\Gamma}) = \text{span}\{\Phi_k(x-y)|_{x \in \Gamma} : y \in \hat{\Gamma}\}.$$

Again, like in Theorem (4.1.9), we point the reader to [35], [39] and [40], where slightly different proofs are stated.

Theorem 4.1.13. *Let Ω be an open and bounded set with C^2 boundary $\Gamma = \partial\Omega$ such that $\overline{\Omega} \subset \hat{\Omega} \subset \mathbb{R}^2$, where $\hat{\Omega}$ is an open and bounded set and $\hat{\Gamma} = \partial\hat{\Omega}$ is an admissible source set. Then, $\mathcal{S}(\Gamma, \hat{\Gamma})$ is dense in $H^{\frac{1}{2}}(\Gamma)$ and in $H^{-\frac{1}{2}}(\Gamma)$.*

Proof. This proof follows the same steps as in the proof of Theorem (4.1.9). Let $E = H^{\frac{1}{2}}(\Gamma)$. For every (fixed) $y \in \hat{\Gamma}$, the map

$$\Phi(\cdot - y) : \varphi \mapsto \int_{\Gamma} \Phi(x-y) \varphi(x) d\sigma(x)$$

is linear and continuous in $H^{\frac{1}{2}}(\Gamma)$ and $\Phi(\cdot - y) \in H^{-\frac{1}{2}}(\Gamma)$. Let $N = \text{span}\{\Phi(\cdot - y)\}$ and

$$N^{\perp} = \{\varphi \in H^{\frac{1}{2}}(\Gamma) : \langle \psi, \varphi \rangle = 0, \psi \in N\}.$$

Once again, we prove that $N^\perp = \{0\}$, i.e, it suffices to prove that given $\varphi \in H^{\frac{1}{2}}(\Gamma)$ the implication

$$\forall y \in \hat{\Gamma}, \int_{\Omega} \Phi(x-y)\varphi(x)d\sigma(x) = 0 \implies \varphi(x) = 0, \forall x \in \mathbb{R}^2$$

holds. Define

$$w(y) = \int_{\Gamma} \Phi(x-y)\varphi(x)d\sigma(x).$$

Given that w satisfies the Sommerfeld Radiation Conditions and, by assumption, $w(y) = 0$ in $\hat{\Gamma}$, then $w = 0$ in Ω is the unique solution of the exterior Dirichlet problem of the Helmholtz equation

$$\begin{cases} -\Delta w = k^2 w, & \text{in } \mathbb{R}^2 \setminus \overline{\Omega} \\ w = 0, & \text{on } \partial\Omega \\ |y|(\frac{y}{|x|} \nabla w(y) - ik)u(x) = 0, & \text{for } |y| \rightarrow \infty, \end{cases}$$

since k is not an eigenfrequency. By analytic continuation, we can extend w by zero to $\mathbb{R}^2 \setminus \overline{\Omega}$. The rest of the proof is the same as in the Theorem (4.1.9), using the fact that k is not an eigenfrequency and the interior Dirichlet problem is well posed. \square

Remark 4.1.14. *Both in Theorem (4.1.9) and Theorem (4.1) the density proof can be generalized to $H^s(\Gamma)$, for $s \geq \frac{1}{2}$. However, in applications, we are only interested in the case $s = \frac{1}{2}$. Regarding Neumann boundary conditions, the proofs above follow the same argument, where one considers the double layer potential $M\varphi$.*

Once again, the discretization argument follows from the linear independence of the functions $\Phi_k(\cdot - y_1), \dots, \Phi_k(\cdot - y_N)$, where $y_1, \dots, y_N \in \mathbb{R}^2 \setminus \overline{\Omega}$ are distinct source points. The proof is identical to the one presented in Theorem (4.1.10), where we use the fact that k is not an eigenfrequency.

Before stating some results regarding the convergence and the stability of the MFS for the Laplace and Helmholtz equations, we address the problem of the source points placement. Although different methods can be considered, e.g. [35], throughout this work we place the artificial boundary $\hat{\Gamma}$ over the boundary of Ω . To be more precise, consider $\Gamma = \partial\Omega$ and the (equally spaced) colocation points $x_1, \dots, x_M \in \Gamma$. Then, we approximate the (outward) normal vector \tilde{n}_i to the point x_i , which is given by

$$\tilde{\mathbf{n}}_i = \frac{(x_i - x_{i-1})^\perp}{2} + \frac{(x_{i+1} - x_i)^\perp}{2},$$

with the orthogonal notation $z^\perp = (-z_2, z_1)$. This way, one can approximate the unit normal vector by $\mathbf{n} = \frac{\tilde{\mathbf{n}}}{|\tilde{\mathbf{n}}|}$ and define the source point y_i by

$$y_i = x_i + \eta \mathbf{n},$$

where $\eta > 0$ is some small coefficient which controls the distance from each point in Γ and $\hat{\Gamma}$. As we shall see below, this coefficient has an important impact on the convergence of the MFS, where bigger values of η produce better approximations. However, this is only feasible for simple geometries, because it also increases the condition number of matrix A , denoted by $\kappa(A)$.

4.2 Numerical approach for the Laplace Equation

Given the results above, it is possible to numerically solve the Laplace and Helmholtz equations for any boundary data $g(x)$ if we are able to find the coefficients in the discretization of the single layer potential. Let N be the number of source points and M the number of colocation points on the boundary, denoted by $x_1, \dots, x_i, \dots, x_M$ with $i = 1, \dots, M$. Then, we solve the discretized equation

$$\tilde{u}(x_i) = \sum_{j=1}^N \alpha_j \Phi(x - y_j) = g(x_i)$$

with respect to the coefficients α_j . Notice that the equation above can be rewritten in the matricial form

$$\underbrace{\begin{bmatrix} \Phi(x_1, y_1) & \cdots & \Phi(x_1, y_N) \\ \vdots & \ddots & \vdots \\ \Phi(x_M, y_1) & \cdots & \Phi(x_M, y_N) \end{bmatrix}}_A \underbrace{\begin{bmatrix} \alpha_1 \\ \vdots \\ \alpha_N \end{bmatrix}}_{\alpha} = \underbrace{\begin{bmatrix} g_1 \\ \vdots \\ g_N \end{bmatrix}}_g \quad (4.4)$$

$M \times N \qquad N \times 1 \qquad M \times 1$

This problem can be framed in two different ways:

- if $N = M$, then we are faced with an interpolation problem, where we solve a linear system of N equations and N unknowns;
- if $M > N$, then we must solve a least-squares problem. Observe that the case $M < N$ is an under determined system of equations and therefore the number of colocation points must be greater than the number of source points. In any case, every numerical linear algebra software is able to solve this type of problem efficiently. This is the method used in this work, since it avoids interpolation instabilities, forces the boundary condition to hold at some specific points and is particularly robust when dealing with non-regular boundary data. After several numerical experiments, e.g. [35], it was concluded that $N = 2M$ is a good choice for the number of source points.

Notice that different boundary conditions can be considered: for example, if solving the Laplace equation with Neumann boundary conditions, one should replace the entries $\Phi(x_i, y_j)$ with $\partial_{n_x} \Phi(x_i, y_j) = \nabla_x \Phi(x_i, y_j) \cdot n$, where n is the unit normal vector to the boundary in the point x_i .

We now state some results regarding the convergence and the stability of the MFS for the Laplace

equation. Here, we state this results when the domain Ω is a disk and the artificial boundary $\hat{\Gamma} = \partial\hat{\Omega}$ that involves Ω is also a circle. Let ρ be the radius of Ω , R the radius of $\hat{\Omega}$ and assume that $N = M$.

Theorem 4.2.1. *Assume that $R^N - \rho^N \neq 1$. Then,*

1. *the matrix A is non-singular;*
2. *if $R \neq 1$ and the boundary data g is real and analytic we can also prove that the exact solution u of the Laplace equation admits a harmonic extension to some neighborhood of $\bar{\Omega}$. Therefore, we may assume that u is harmonic in $0 \leq r \leq r_0$ for some $r_0 \geq \rho$. In this case, there exists $C > 0$ and $c \in (0, 1)$ which are independent of N and u such that*

$$\sup_{x \in \bar{\Omega}} |u(x) - \tilde{u}(x)| \leq Cc^N \sup_{|x| \leq r_0} |u(x)|.$$

The Theorem above provides some important insights regarding the MFS. First, we cannot fail to notice that this method displays *exponential convergence* in the number of source points, which is quite remarkable. In fact, the term c depends on the distance between Γ and the artificial boundary $\hat{\Gamma}$, which is controlled by the coefficient η , and

$$c = \begin{cases} \frac{\rho}{R}, & \text{if } r_0 > \frac{R^2}{\rho} \\ \sqrt{\frac{\rho}{R}}, & \text{if } r_0 < \frac{R^2}{\rho}. \end{cases}$$

Unfortunately, one of the main drawbacks of the MFS is the ill-condition of the matrix A and the fact that the matrix A is very dense, and we cannot use optimized sparse software solvers on the system (4.4). In particular, while bigger values of the parameter η allows for better numerical approximations it also implies an exponential growth of the condition number $\kappa(A)$, see [41], [42] and [43].

Theorem 4.2.2. *In the conditions of the Theorem (4.2.1), the condition number can be estimated by*

$$\kappa(A) \sim \frac{\log R}{2} N \left(\frac{R}{\rho} \right)^{\frac{N}{2}}.$$

Another interesting remark, is the condition $R \neq 1$, which is in direct connection with the space $S(\Gamma, \hat{\Gamma}) \oplus \mathbb{R}$ that was proven to be dense in $H^{\frac{1}{2}}(\Gamma)$ in Theorem (4.1.9). Assume that $R = 1$ and $\hat{\Omega}$ is a disk with radius R that contains the origin. Then,

$$\tilde{u}(0) = \sum_{j=1}^N \alpha_j \Phi(0 - y_j) = -\frac{1}{2\pi} \sum_{j=1}^N \alpha_j \log(R) = 0,$$

no matter the choice of the source points over $\hat{\Gamma}$. Therefore, it is impossible to approximate any harmonic function which does not vanish on the origin. However, this is not the case if we add the basis function

1, which was used to prove the density result. While this almost never interferes with the numerical approximations in the next chapters, it will be considered nevertheless by a reason of coherence.

4.2.1 An enrichment technique

Before diving into the numerical approach for the Helmholtz equation, we introduce some modifications to the classical MFS method presented above. There is another drawback in our method: our basis functions are analytical and might lose precision when approximating functions which display singularities, for example near a corner if the domain is not smooth. In what follows we introduce an enrichment technique which allows for singularity treatment. In the same vein as in the Proposition (3.2.3), we reintroduce the notion of a wedge domain and consider some wedge like domain with interior angle Θ .

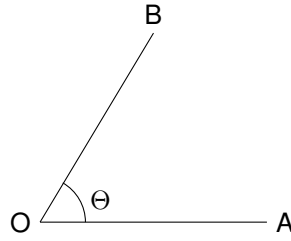


Figure 4.1: A wedge domain with an interior angle Θ .

Consider the Laplace equation in polar coordinates, given by

$$\left(\partial_r^2 + \frac{1}{r} \partial_r + \frac{1}{r^2} \partial_\theta^2 \right) u(r, \theta) = 0, \quad r > 0, \quad 0 \leq \theta \leq \Theta. \quad (4.5)$$

Then, by separation of variables $u(r, \theta) = R(r)T(\theta)$, one can find two different families of particular solutions given by,

$$u(r, \theta) = (c_1 r^\alpha + c_2 r^{-\alpha}) \times (c_3 \cos(\alpha\theta) + c_4 \sin(\alpha\theta)), \quad \alpha > 0$$

and

$$u(r, \theta) = (c_1 \log(r) + c_2) \times (c_3 \cos(\alpha\theta) + c_4 \sin(\alpha\theta)), \quad \alpha = 0$$

where $c_1, c_2, c_3, c_4 \in \mathbb{C}$. In order to find α , one must consider the amplitude of the angle Θ and the boundary conditions at each segment \overrightarrow{OA} and \overrightarrow{OB} . Below we summarize the asymptotic harmonic solutions of (4.5). For more details we point the reader to [1].

- For Dirichlet-Dirichlet boundary conditions given by $u(r, 0) = A, u(r, \Theta) = B$, then $\alpha_k = \frac{k\pi}{\Theta}$ and

$$u(r, \theta) = A(B - A) \frac{\theta}{\Theta} + \sum_{k=0}^{\infty} \alpha_k r^{\alpha_k} \sin(\alpha_k \theta);$$

- For Dirichlet-Neumann boundary conditions given by $u(r, 0) = A$, $\partial_n u(r, \Theta) = B$, then $\alpha_k = \frac{(k+\frac{1}{2})\pi}{\Theta}$ and

- If $\Theta \neq \frac{\pi}{2}, \frac{3\pi}{2}$,

$$u(r, \theta) = A + \frac{B}{\cos(\Theta)} r \sin(\theta) + \sum_{k=0}^{\infty} \alpha_k r^{\alpha_k} \sin(\alpha_k \theta);$$

- If $\Theta = \frac{\pi}{2}, \frac{3\pi}{2}$,

$$u(r, \theta) = A + (-1)^{l+1} \frac{Br}{\Theta} (\log(r) \sin(\theta) + \theta \cos(\theta)) + \sum_{k=0}^{\infty} \alpha_k r^{\alpha_k} \sin(\alpha_k \theta),$$

with $l = 0$ if $\Theta = \frac{\pi}{2}$ and $l = 1$ if $\Theta = \frac{3\pi}{2}$;

- For Neumann-Dirichlet boundary conditions given by $\partial_n u(r, 0) = A$, $u(r, \Theta) = B$, then $\alpha_k = \frac{(k+\frac{1}{2})\pi}{\Theta}$ and

- If $\Theta \neq \frac{\pi}{2}, \frac{3\pi}{2}$,

$$u(r, \theta) = B - Ar \sin(\theta) + \frac{A \sin(\Theta)}{\cos(\Theta)} r \cos(\theta) + \sum_{k=0}^{\infty} \alpha_k r^{\alpha_k} \cos(\alpha_k \theta);$$

- If $\Theta = \frac{\pi}{2}, \frac{3\pi}{2}$,

$$u(r, \theta) = B - \frac{Ar}{\Theta} (\log(r) \cos(\theta) - \theta \sin(\theta)) - Ar \sin(\theta) + \sum_{k=0}^{\infty} \alpha_k r^{\alpha_k} \cos(\alpha_k \theta);$$

- For Neumann-Neumann boundary conditions given by $\partial_n u(r, 0) = A$, $\partial_n u(r, \Theta) = B$, then $\alpha_k = \frac{k\pi}{\Theta}$ and

- If $\Theta \neq \pi, 2\pi$,

$$u(r, \theta) = -Ar \sin(\theta) - \frac{B + A \cos(\Theta)}{\sin(\Theta)} r \cos(\theta) + \sum_{k=0}^{\infty} \alpha_k r^{\alpha_k} \cos(\alpha_k \theta);$$

- If $\Theta = \pi, 2\pi$,

$$u(r, \theta) = -Ar \sin(\theta) + \frac{(-1)^l B - A}{\Theta} r (\log(r) \cos(\theta) - \theta \sin(\theta)) + \sum_{k=0}^{\infty} \alpha_k r^{\alpha_k} \cos(\alpha_k \theta);$$

with $l = 0$ if $\Theta = \pi$ and $l = 1$ if $\Theta = 2\pi$.

Remark 4.2.3. Observe that if the wedge domain is rotated by some angle θ_1 (see Figure (4.2)) one can consider the translation $\theta^* = \theta - \theta_1$, where θ^* is the angle on the "correct" wedge domain, see Figure

(4.1).

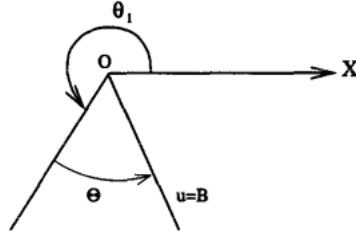


Figure 4.2: Rotation of the wedge domain. Image taken from [1].

In applications, we are mostly concerned with Dirichlet-Dirichlet, Dirichlet-Neumann and Neumann-Dirichlet boundary conditions. Just like stated above, some of these boundary conditions have different expansions for the angles $\Theta = \frac{\pi}{2}$ and $\Theta = \frac{3\pi}{2}$. However, we are only concerned with the expansion

$$v(r, \theta) = \sum_{k=0}^{\infty} \alpha_k r^{\alpha_k} \psi(\alpha_k \theta)$$

where $\psi = \sin$ or $\psi = \cos$. In these cases, if we neglect the other terms, for the special angle $\Theta = \frac{\pi}{2}$ above we would find that $\alpha_k \in \mathbb{N}$. Without going in dept in singularity analysis, then its partial derivative $\partial_r v(r, \theta)$ would be of the form

$$\partial_r v(r, \theta) = \sum_{k=0}^{\infty} \alpha_k^2 r^{\alpha_k - 1} \psi(\alpha_k \theta)$$

where $\alpha_k - 1 \in \mathbb{N}$. In general, if $\alpha_k \in \mathbb{N}$ for some angle Θ then all of its derivatives are continuous and $v(r, \theta)$ is analytical. More precisely, there is no singularity in these cases. Therefore, one does not need to enrich the set of basis functions since the fundamental solutions correctly reproduce the behavior near the corner's tip. Such corners are called regular. On the other hand, corners which present singularities are called singular and are the ones which we are interested to better approximate.

Also notice that, in the expansions above, the term $r^{-\alpha_k}$ does not appear. This has to do with the fact we are dealing with an interior problem: when considering the exterior problem, the terms r^{α_k} are replaced with $r^{-\alpha_k}$ (observe that it satisfies the asymptotic conditions prescribed in order to have well-posedness!).

To incorporate the singular behavior near a singular corner, first assume, without loss of generality, that the domain Ω has just one corner and that the solution of our BVP can be decomposed in regular and singular parts,

$$u(x) = u_R(x) + u_S(x), \quad x \in \overline{\Omega},$$

where u_R is the regular part is approximated by the MFS basis functions, and the singular part u_S is approximated by the expansions above, having the boundary conditions into account. Let $\phi_s(r, \theta)$ be

one of those expansions centered at the corner's tip, where s is the order of the expansion. Then, the numerical approximation can be written as

$$\tilde{u}(x) = \sum_{j=1}^N \alpha_j \Phi(x - y_j) + \sum_{s=1}^p \beta_s \phi_s(r(x), \theta(x)), \quad x \in \overline{\Omega}. \quad (4.6)$$

Considering the collocation points $x_1, \dots, x_M \in \partial\Omega$, the linear system of equations (4.4) can be generalized to

$$\begin{bmatrix} A_1 & B_1 \end{bmatrix}_{M \times (N+P)} \begin{bmatrix} \alpha \\ \beta \end{bmatrix}_{(N+P) \times 1} = \begin{bmatrix} g \end{bmatrix}_{M \times 1}, \quad (4.7)$$

where the block matrix A_1 is the matrix A in (4.4) and the B_1 block matrix is given by

$$B_1 = \begin{bmatrix} \phi_1(r(x_1), \theta(x_1)) & \cdots & \phi_p(r(x_1), \theta(x_1)) \\ \vdots & \ddots & \vdots \\ \phi_1(r(x_M), \theta(x_M)) & \cdots & \phi_p(r(x_M), \theta(x_M)) \end{bmatrix}$$

4.3 Numerical approach for the Helmholtz Equation

For the Helmholtz equation, the MFS convergence and stability results resemble the previous ones for the Laplace equation. Once again, the results are stated for identical geometries as before, where Ω is the unit disk and the radius of $\hat{\Omega}$ is $R > 1$. Here is assumed that the boundary data g can be analytically extended to the annulus $\{z \in \mathbb{C} : \frac{1}{\rho} < |z| < \rho\}$, where $\rho > 1$. The following result is due to [44].

Theorem 4.3.1. *Let $R > 1$ and N be an even number. Then the minimum boundary error achieved by the MFS in the unit disk satisfies*

$$\|g - \tilde{u}|_{\Gamma}\|_{L^2(\Gamma)} \leq \begin{cases} C\rho^{-\frac{N}{2}}, & \text{if } \rho < R^2 \\ C\sqrt{N}R^{-N}, & \text{if } \rho = R^2 \\ CR^{-N}, & \text{if } \rho > R^2 \end{cases}$$

where C is a constant that not depends on N .

To solve the Helmholtz equation with the MFS, one must start by computing the eigenvalues λ (or the eigenfrequencies k , with $\lambda = k^2$) first. In order to achieve that, recall that the Helmholtz equation

$$\begin{cases} -\Delta u = \lambda u, & \text{in } \Omega \\ \mathcal{B}u = 0, & \text{on } \partial\Omega \end{cases}$$

is well-posed when prescribing boundary conditions given by \mathcal{B} , and if λ is not an eigenvalue. Observe that if λ is not an eigenvalue of the Laplace Operator, then $N(-(\Delta + \lambda I)) = \{0\}$ and the nullspace of

the single layer potential operator

$$S_k \varphi(y) = \int_{\hat{\Gamma}} \Phi_k(x-y) \varphi(x) d\sigma(x)$$

is trivial. More precisely, one can prove the following result, e.g. [45].

Theorem 4.3.2. *If k is not an eigenfrequency of the interior Dirichlet problem, then $\dim N(S_k) = 0$.*

Proof. If k is not an eigenfrequency, then the interior problem is well posed which implies that $\varphi(x) = 0$, $x \in \overline{\Omega}$. By analytical continuation, $\varphi(x) = 0$, $x \in \hat{\Omega}$. Since the single layer potential is continuous, then $\varphi(x) = 0$, $x \in \hat{\Gamma}$. By the well-posedness of the exterior problem (notice that the single layer potential satisfies the Sommerfeld radiation conditions), then $\varphi(x) = 0$, $\forall x \in \mathbb{R}^2$. \square

The theorem can be used to search for the eigenvalues/eigenfrequencies of the Laplace operator. By virtue of the discretization of the single layer potential (4.1), one should find the values k such that the nullspace of the matrix $A(k) = [\Phi_k(x_i - y_j)]_{M \times N}$ is not trivial. Like it was discussed in the previous section 4.2, that can be done in two different ways:

1. if $A(k)$ is a square matrix (with $M = N$), one can compute the determinant of $A(k)$. Since the components of $A(k)$ are complex numbers, then its determinant is also a complex number, and we consider its absolute value. In any case, instead of working with $|\det A(k)|$, since this value is very small, one must work with its logarithm and consider the function $d(k) = \log |\det A(k)|$;
2. if $A(k)$ is an $M \times N$ rectangular matrix, with $M > N$, one considers the smallest singular value, which we denote by $\sigma_N(k)$, where the singular values of $A(k)$ are assumed to be in decreasing order $\sigma_1(k) \geq \dots \geq \sigma_N(k)$. We emphasize that we only work with this case.

Therefore, in order to find the eigenvalues/eigenfrequencies of the Laplace operator, one must find the singularities of the functions $d(k)$ or $\sigma_N(k)$ for the first and second cases above, respectively.

4.3.1 The Subspace Angle Technique

5

Conducted Numerical Simulations

Contents

5.1	Poisson Equation using MFS-B	56
5.2	Poisson Equation using MFS-D	57
5.3	Helmholtz Equation using MFS-B	57
5.3.1	User Interface	58
5.3.2	Vivamus luctus elit sit amet mi	58
5.4	Helmholtz Equation in Rectangular Domains using MFS-B	60
5.5	Helmholtz Equation in Rectangular Domains using MFS-D	60
5.6	Dirac Operator Spectrum in Rectangular Domains using MFS-B	60
5.7	Dirac Operator Spectrum in Rectangular Domains using MFS-D	60
5.8	Dirac Operator Spectrum in General Polygonal Domains using MFS-D	60

Aliquam aliquet, est a ullamcorper condimentum, tellus nulla fringilla elit, a iaculis nulla turpis sed wisi. Fusce volutpat. Etiam sodales ante id nunc. Proin ornare dignissim lacus. Nunc porttitor nunc a sem. Sed sollicitudin velit eu magna. Aliquam erat volutpat. Vivamus ornare est non wisi. Proin vel quam. Vivamus egestas. Nunc tempor diam vehicula mauris. Nullam sapien eros, facilisis vel, eleifend non, auctor dapibus, pede.

5.1 Poisson Equation using MFS-B

Suspendisse vestibulum dignissim quam. Integer vel augue. Phasellus nulla purus, interdum ac, venenatis non, varius rutrum, leo. Pellentesque habitant morbi tristique senectus et netus et malesuada fames ac turpis egestas. Duis a eros. Class aptent taciti sociosqu ad litora torquent per conubia nostra, per inceptos hymenaeos. Fusce magna mi, porttitor quis, convallis eget, sodales ac, urna. Phasellus luctus venenatis magna. Vivamus eget lacus. Nunc tincidunt convallis tortor. Duis eros mi, dictum vel, fringilla sit amet, fermentum id, sem. Phasellus nunc enim, faucibus ut, laoreet in, consequat id, metus. Vivamus dignissim. Cras lobortis tempor velit. Phasellus nec diam ac nisl lacinia tristique. Nullam nec metus id mi dictum dignissim. Nullam quis wisi non sem lobortis condimentum. Phasellus pulvinar, nulla non aliquam eleifend, tortor wisi scelerisque felis, in sollicitudin arcu ante lacinia leo.:

- Technology Research and Related Works
- Requirements Gathering and Study
- Design of the Architecture
- Implementation Process
- Testing and Functional Validation

Pellentesque nibh felis, eleifend id, commodo in, interdum vitae, leo. Praesent eu elit. Ut eu ligula. Class aptent taciti sociosqu ad litora torquent per conubia nostra, per inceptos hymenaeos. Maecenas elementum augue nec nisl. Proin auctor lorem at nibh. Curabitur nulla purus, feugiat id, elementum in, lobortis quis, pede. Vivamus sodales adipiscing sapien. Vestibulum posuere nulla eget wisi. Integer volutpat ligula eget enim. Suspendisse vitae arcu. Quisque pellentesque. Nullam consequat, sem vitae rhoncus tristique, mauris nulla fermentum est, bibendum ullamcorper sapien magna et quam. Sed dapibus vehicula odio. Proin bibendum gravida nisl. Fusce lorem. Phasellus sagittis, nulla in hendrerit laoreet, libero lacus feugiat urna, eget hendrerit pede magna vitae lorem. Praesent mauris.

5.2 Poisson Equation using MFS-D

Cras sed ante. Phasellus in massa. Curabitur dolor eros, gravida et, hendrerit ac, cursus non, massa. Aliquam lorem. In hac habitasse platea dictumst. Cras eu mauris Algorithm 5.1. Quisque lacus. Donec ipsum. Nullam vitae sem at nunc pharetra ultricies. Vivamus elit eros, ullamcorper a, adipiscing sit amet, porttitor ut, nibh.

RC
Notice the
reference
to the AI-
gorithm
construct

Algorithm 5.1: Time Control Strategy

```
begin
  nextBitrate  $\leftarrow$  nextDownloadLevel
  nextBitrate  $\leftarrow$  GetNextBitrate()
  cpuLoad  $\leftarrow$  GetCpuLoad()
  bitrateDelta  $\leftarrow$  getBitrateDelta(currentBitrate, nextBitrate)

  if bitrateDelta > maxThreshold then
    | SetBitrate(nextBitrate)

  if minThreshold < bitrateDelta < maxThreshold and numAttempts < 2 then
    | numAttempts  $\leftarrow$  numAttempts + 1
  else if minThreshold < bitrateDelta < maxThreshold and numAttempts = 2 then
    | numAttempts  $\leftarrow$  0
  else
    | SetBitrate(nextBitrate)
  if 0 < bitrateDelta < minThreshold and numAttempts < 3 then
    | numAttempts  $\leftarrow$  numAttempts + 1
  else if 0 < bitrateDelta < minThreshold and numAttempts = 3 then
    | SetBitrate(nextBitrate)
```

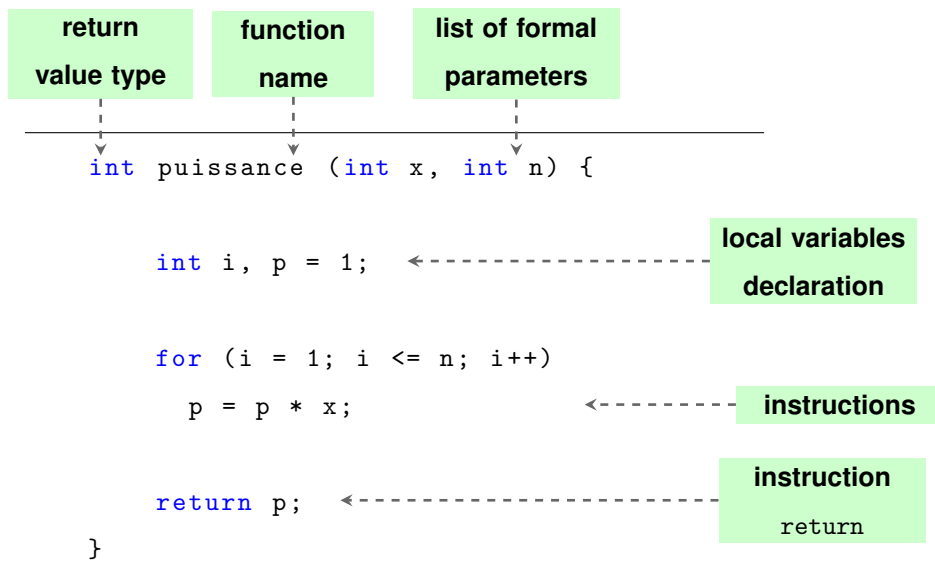
Maecenas adipiscing mollis massa. Nunc ut dui eget nulla venenatis aliquet. Sed luctus posuere justo. Cras vehicula varius turpis. Vivamus eros metus, tristique sit amet, molestie dignissim, malesuada et, urna..

5.3 Helmholtz Equation using MFS-B

Cras sed ante. Phasellus in massa. Curabitur dolor eros, gravida et, hendrerit ac, cursus non, massa. Aliquam lorem. In hac habitasse platea dictumst. Cras eu mauris. Quisque lacus. Donec ipsum. Nullam vitae sem at nunc pharetra ultricies.

Vivamus elit eros, ullamcorper a, adipiscing sit amet, porttitor ut, nibh. Maecenas adipiscing mollis massa. Nunc ut dui eget nulla venenatis aliquet. Sed luctus posuere justo. Cras vehicula varius turpis. Vivamus eros metus, tristique sit amet, molestie dignissim, malesuada et, urna.

Quisque lacus. Donec ipsum. Nullam vitae sem at nunc pharetra ultricies. Cras vehicula varius turpis.



Listagem 5.1: A listing with a Tikz picture overlaid

And here another method (Listing 5.1) for mixing (overlay) a picture with a listing of code.

5.3.1 User Interface

Donec semper turpis sed diam. Sed consequat ligula nec tortor. Integer eget sem. Ut vitae enim eu est vehicula gravida. Morbi ipsum ipsum, porta nec, tempor id, auctor vitae, purus. Pellentesque neque. Nulla luctus erat vitae libero. Integer nec enim. Phasellus aliquam enim et tortor. Quisque aliquet, quam elementum condimentum feugiat, tellus odio consectetur wisi, vel nonummy sem neque in elit. Curabitur eleifend wisi iaculis ipsum. Pellentesque habitant morbi tristique senectus et netus et malesuada fames ac turpis egestas. In non velit non ligula laoreet ultrices. Praesent ultricies facilisis nisl. Vivamus luctus elit sit amet mi. Phasellus pellentesque, erat eget elementum volutpat, dolor nisl porta neque, vitae sodales ipsum nibh in ligula. Maecenas mattis pulvinar diam. Curabitur sed leo..

Cras eu mauris. Quisque lacus. Donec ipsum. Nullam vitae sem at nunc pharetra ultricies. Vivamus elit eros, ullamcorper a, adipiscing sit amet, porttitor ut, nibh. Maecenas adipiscing mollis massa. Nunc ut dui eget nulla venenatis aliquet. Sed luctus posuere justo. Cras vehicula varius turpis.

5.3.2 Vivamus luctus elit sit amet mi

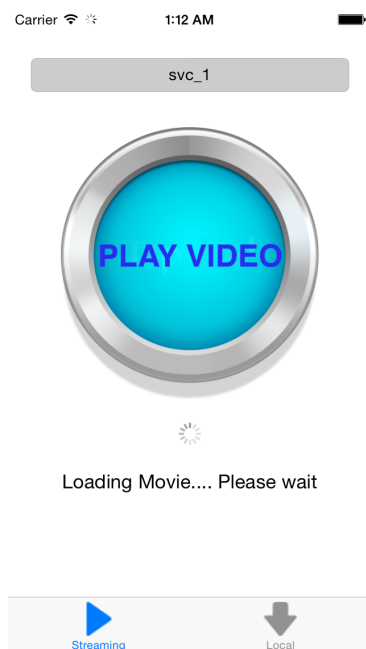
Nulla facilisi. In vel sem. Morbi id urna in diam dignissim feugiat. Proin molestie tortor eu velit. Aliquam erat volutpat. Nullam ultrices, diam tempus vulputate egestas, eros pede varius leo, sed imperdiet lectus est ornare odio. Lorem ipsum dolor sit amet, consectetur adipiscing elit. Proin consectetur velit in dui. Phasellus wisi purus, interdum vitae, rutrum accumsan, viverra in, velit. Sed enim risus, congue non, tristique in, commodo eu, metus. Aenean tortor mi, imperdiet id, gravida eu, posuere eu, felis.

Mauris sollicitudin, turpis in hendrerit sodales, lectus ipsum pellentesque ligula, sit amet scelerisque

urna nibh ut arcu. Aliquam in lacus.

Figures 5.1(a) and 5.1(b) proin at eros non eros adipiscing mollis.

RC
A figure
with Subfig-
ures



(a) Media Loading Window



(b) Play-out Session UI

Figure 5.1: Complete User Interface

Vestibulum ante ipsum primis in User Interface (UI) faucibus orci luctus et ultrices posuere cubilia Curae; Nulla placerat aliquam wisi. Mauris viverra odio. Quisque fermentum pulvinar odio. Proin posuere est vitae ligula. Etiam euismod. Cras a eros.

5.4 Helmholtz Equation in Rectangular Domains using MFS-B

5.5 Helmholtz Equation in Rectangular Domains using MFS-D

5.6 Dirac Operator Spectrum in Rectangular Domains using MFS-B

5.7 Dirac Operator Spectrum in Rectangular Domains using MFS-D

5.8 Dirac Operator Spectrum in General Polygonal Domains using MFS-D

6

The Poisson Equation with Variable Coefficients

Contents

6.1	Maecenas vitae nulla consequat	62
6.2	Proin ornare dignissim lacus	63

Lorem ipsum dolor sit amet, consectetur adipiscing elit. Morbi commodo, ipsum sed pharetra gravida, orci magna rhoncus neque, id pulvinar odio lorem non turpis. Nullam sit amet enim. Suspendisse id velit vitae ligula volutpat condimentum. Aliquam erat volutpat. Sed quis velit. Nulla facilisi. Nulla libero. Vivamus pharetra posuere sapien. Nam consectetur. Sed aliquam, nunc eget euismod ullamcorper, lectus nunc ullamcorper orci, fermentum bibendum enim nibh eget ipsum. Donec porttitor ligula eu dolor. Maecenas vitae nulla consequat libero cursus venenatis. Nam magna enim, accumsan eu, blandit sed, blandit a, eros.

6.1 Maecenas vitae nulla consequat

Aliquam aliquet, est a ullamcorper condimentum, tellus nulla fringilla elit, a iaculis nulla turpis sed wisi. Fusce volutpat. Etiam sodales ante id nunc. Proin ornare dignissim lacus. Nunc porttitor nunc a sem. Sed sollicitudin velit eu magna. Aliquam erat volutpat. Vivamus ornare est non wisi. Proin vel quam. Vivamus egestas. Nunc tempor diam vehicula mauris. Nullam sapien eros Figure 6.1, facilisis vel, eleifend non, auctor dapibus, pede.

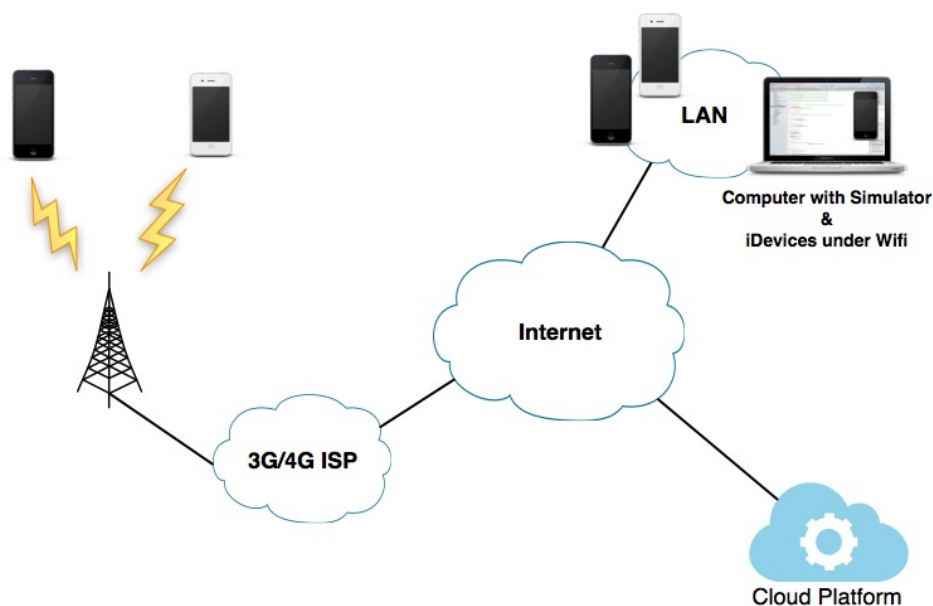


Figure 6.1: Test Environment

Aliquam aliquet, est a ullamcorper condimentum, tellus nulla fringilla elit, a iaculis nulla turpis sed wisi. Fusce volutpat. Etiam sodales ante id nunc. Proin ornare dignissim lacus. Nunc porttitor nunc a sem. Sed sollicitudin velit eu magna. Aliquam erat volutpat. Vivamus egestas. Nunc tempor diam vehicula mauris. Nullam sapien eros, facilisis vel, eleifend non, auctor dapibus, pede Table 6.1 used in the tests. The Network Link Conditioner allows to force/simulate fluctuations in fixed network segments.

Table 6.1: Network Link Conditioner Profiles

Network Profile	Bandwidth	Packets Dropped	Delay
Wifi	40 mbps	0%	1 ms
3G	780 kbps	0%	100 ms
Edge	240 kbps	0%	400 ms

Aliquam aliquet, est a ullamcorper condimentum, tellus nulla fringilla elit, a iaculis nulla turpis sed wisi. Fusce volutpat. Etiam sodales ante id nunc. Proin ornare dignissim lacus. Nunc porttitor nunc a sem. Sed sollicitudin velit eu magna. Aliquam erat volutpat. Vivamus ornare est non wisi. Proin vel quam. Vivamus egestas. Nunc tempor diam vehicula mauris. Nullam sapien eros, facilisis vel, eleifend non, auctor dapibus, pede.

6.2 Proin ornare dignissim lacus

Pellentesque habitant morbi tristique senectus et netus et malesuada fames ac turpis egestas. Vestibulum tortor quam, feugiat vitae, ultricies eget, tempor sit amet, ante. Donec eu libero sit amet quam egestas semper. Aenean ultricies mi vitae est. Mauris placerat eleifend leo. Quisque sit amet est et sapien ullamcorper pharetra. Vestibulum erat wisi, condimentum sed, commodo vitae, ornare sit amet, wisi. Aenean fermentum, elit eget tincidunt condimentum, eros ipsum rutrum orci, sagittis tempus lacus enim ac dui. Donec non enim in turpis pulvinar facilisis. Ut felis.

Et “optimistic” nulla dui purus, eleifend vel, consequat non, dictum porta, nulla. Duis ante mi, laoreet ut, commodo eleifend, cursus nec, lorem. Aenean eu est. Etiam imperdiet turpis. Praesent nec augue. Curabitur ligula quam, rutrum id, tempor sed, consequat ac, dui G_j , nec ligula et lorem consequat ullamcorper p ut mauris eu mi mollis luctus j , porttitor ut, Equation (6.1), uctus posuere justo:

N_j Is the number of times peer j has been optimistically unchoked.

n_j Among the N_j unchokes, the number of times that peer j responded with unchoke or supplied segments to peer p .

$C_{r[j]}$ The cooperation ratio of peer j . If peer j never supplied peer p , the information of $C_{r[j]}$ may not be available.

$C_{r(max)}$ The maximum cooperation ratio of peer p 's neighbors, i.e., $C_{r(max)} = \max(C_r)$.

$$G_j = \begin{cases} \frac{n_j C_{r[j]}}{N_j} & \text{if } n_j > 0 \\ \frac{C_{r(max)}}{N_j + 1} & \text{if } n_j = 0 \end{cases} \quad (6.1)$$

Cursus $C_{r(max)}$ conubia nostra, per inceptos hymenaeos j gadipiscing mollis massa $N_j = 0$, unc ut dui eget nulla venenatis aliquet $G_j = C_{r(max)}$.

Vestibulum accumsan eros nec magna. Vestibulum vitae dui. Vestibulum nec ligula et lorem consequat ullamcorper. Class aptent taciti sociosqu ad litora torquent per conubia nostra, per inceptos hymenaeos. Phasellus eget nisl ut elit porta ullamcorper. Maecenas tincidunt velit quis orci. Sed in dui. Nullam ut mauris eu mi mollis luctus. Class aptent taciti sociosqu ad litora torquent per conubia nostra, per inceptos hymenaeos. Sed cursus cursus velit. Sed a massa.

Both Figures 6.2(a) and 6.2(b) Phasellus eget nisl ut elit porta “perfect” tincidunt. Class aptent taciti sociosqu ad litora torquent per conubia nostra.

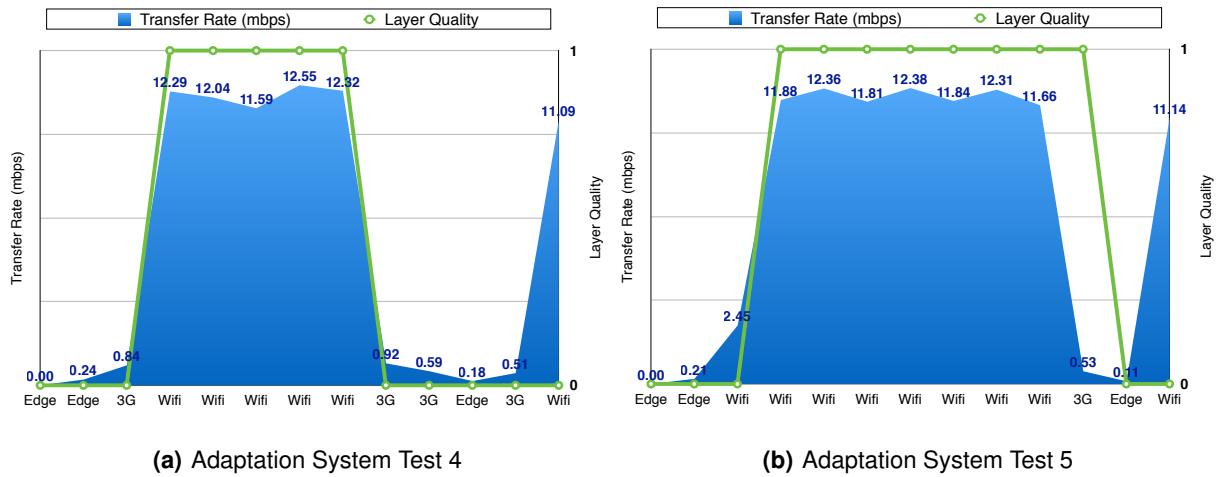


Figure 6.2: Adaptation System Behavior Test

Cras sed ante. Phasellus in massa. Curabitur dolor eros, gravida et, hendrerit ac, cursus non, massa. Aliquam lorem. In hac habitasse platea dictumst. Cras eu mauris. Quisque lacus. Donec ipsum. Nullam vitae sem at nunc pharetra ultricies. Vivamus elit eros, ullamcorper a, adipiscing sit amet, porttitor ut, nibh. Maecenas adipiscing mollis massa. Nunc ut dui eget nulla venenatis aliquet. Sed luctus posuere justo. Cras vehicula varius turpis. Vivamus eros metus, tristique sit amet, molestie dignissim, malesuada et, urna.

7

Conclusion

Contents

7.1	Conclusions	66
7.2	System Limitations and Future Work	67

Pellentesque vel dui sed orci faucibus iaculis. Suspendisse dictum magna id purus tincidunt rutrum. Nulla congue. Vivamus sit amet lorem posuere dui vulputate ornare. Phasellus mattis sollicitudin ligula. Duis dignissim felis et urna. Integer adipiscing congue metus.

7.1 Conclusions

Lorem ipsum dolor sit amet, consectetur adipiscing elit. Morbi commodo, ipsum sed pharetra gravida, orci magna rhoncus neque, id pulvinar odio lorem non turpis. Nullam sit amet enim. Suspendisse id velit vitae ligula volutpat condimentum. Aliquam erat volutpat. Sed quis velit. Nulla facilisi. Nulla libero. Vivamus pharetra posuere sapien. Nam consectetur. Sed aliquam, nunc eget euismod ullamcorper, lectus nunc ullamcorper orci, fermentum bibendum enim nibh eget ipsum. Donec porttitor ligula eu dolor. Maecenas vitae nulla consequat libero cursus venenatis. Nam magna enim, accumsan eu, blandit sed, blandit a, eros.

Quisque facilisis erat a dui. Nam malesuada ornare dolor. Cras gravida, diam sit amet rhoncus ornare, erat elit consectetur erat, id egestas pede nibh eget odio. Proin tincidunt, velit vel porta elementum, magna diam molestie sapien, non aliquet massa pede eu diam. Aliquam iaculis. Fusce et ipsum et nulla tristique facilisis. Donec eget sem sit amet ligula viverra gravida. Etiam vehicula urna vel turpis. Suspendisse sagittis ante a urna. Morbi a est quis orci consequat rutrum. Nullam egestas feugiat felis. Integer adipiscing semper ligula. Nunc molestie, nisl sit amet cursus convallis, sapien lectus pretium metus, vitae pretium enim wisi id lectus. Donec vestibulum. Etiam vel nibh. Nulla facilisi. Mauris pharetra. Donec augue. Fusce ultrices, neque id dignissim ultrices, tellus mauris dictum elit, vel lacinia enim metus eu nunc.

Proin at eros non eros adipiscing mollis. Donec semper turpis sed diam. Sed consequat ligula nec tortor. Integer eget sem. Ut vitae enim eu est vehicula gravida. Morbi ipsum ipsum, porta nec, tempor id, auctor vitae, purus. Pellentesque neque. Nulla luctus erat vitae libero. Integer nec enim. Phasellus aliquam enim et tortor. Quisque aliquet, quam elementum condimentum feugiat, tellus odio consectetur wisi, vel nonummy sem neque in elit. Curabitur eleifend wisi iaculis ipsum. Pellentesque habitant morbi tristique senectus et netus et malesuada fames ac turpis egestas. In non velit non ligula laoreet ultrices. Praesent ultricies facilisis nisl. Vivamus luctus elit sit amet mi. Phasellus pellentesque, erat eget elementum volutpat, dolor nisl porta neque, vitae sodales ipsum nibh in ligula. Maecenas mattis pulvinar diam. Curabitur sed leo.

Nulla facilisi. In vel sem. Morbi id urna in diam dignissim feugiat. Proin molestie tortor eu velit. Aliquam erat volutpat. Nullam ultrices, diam tempus vulputate egestas, eros pede varius leo, sed imperdiet lectus est ornare odio. Lorem ipsum dolor sit amet, consectetur adipiscing elit. Proin consectetur velit in dui. Phasellus wisi purus, interdum vitae, rutrum accumsan, viverra in, velit. Sed enim risus, congue

non, tristique in, commodo eu, metus. Aenean tortor mi, imperdiet id, gravida eu, posuere eu, felis. Mauris sollicitudin, turpis in hendrerit sodales, lectus ipsum pellentesque ligula, sit amet scelerisque urna nibh ut arcu. Aliquam in lacus. Vestibulum ante ipsum primis in faucibus orci luctus et ultrices posuere cubilia Curae; Nulla placerat aliquam wisi. Mauris viverra odio. Quisque fermentum pulvinar odio. Proin posuere est vitae ligula. Etiam euismod. Cras a eros.

Nunc auctor bibendum eros. Maecenas porta accumsan mauris. Etiam enim enim, elementum sed, bibendum quis, rhoncus non, metus. Fusce neque dolor, adipiscing sed, consectetur et, lacinia sit amet, quam.

7.2 System Limitations and Future Work

Aliquam aliquet, est a ullamcorper condimentum, tellus nulla fringilla elit, a iaculis nulla turpis sed wisi. Fusce volutpat. Etiam sodales ante id nunc. Proin ornare dignissim lacus. Nunc porttitor nunc a sem. Sed sollicitudin velit eu magna. Aliquam erat volutpat. Vivamus ornare est non wisi. Proin vel quam. Vivamus egestas. Nunc tempor diam vehicula mauris. Nullam sapien eros, facilisis vel, eleifend non, auctor dapibus, pede.

Bibliography

- [1] Z.-C. Li and T.-T. Lu, “Singularities and treatments of elliptic boundary value problems,” *Mathematical and Computer Modelling*, vol. 31, no. 8-9, pp. 97–145, 2000.
- [2] W. Rudin, *Functional Analysis*, ser. International series in pure and applied mathematics. McGraw-Hill, 1991. [Online]. Available: https://books.google.pt/books?id=Sh_vAAAAMAAJ
- [3] H. Brezis and H. Brézis, *Functional analysis, Sobolev spaces and partial differential equations*. Springer, 2011, vol. 2, no. 3.
- [4] W. Arendt and K. Urban, *Partielle differenzialgleichungen*. Springer, 2010.
- [5] J. L. Lions and E. Magenes, *Non-homogeneous boundary value problems and applications: Vol. 1*. Springer Science & Business Media, 2012, vol. 181.
- [6] H. Tavares, “Partial differential equations, lecture notes,” https://ulisboa-my.sharepoint.com/:b:/g/personal/ist27898_tecnico_ulisboa_pt/EfizUpSVmCRCo0Nst2a-sacBDwFrkPuh9w8A55EU9BoFmA?e=kY5B2R.
- [7] L. C. Evans, *Partial differential equations*. American Mathematical Society, 2022, vol. 19.
- [8] A. Bogomolny, “Fundamental solutions method for elliptic boundary value problems,” *SIAM Journal on Numerical Analysis*, vol. 22, no. 4, pp. 644–669, 1985.
- [9] S. N. Chandler-Wilde, D. P. Hewett, and A. Moiola, “Sobolev spaces on non-lipschitz subsets of \mathbb{R}^n with application to boundary integral equations on fractal screens,” *Integral Equations and Operator Theory*, vol. 87, no. 2, pp. 179–224, 2017.
- [10] D. P. Hewett and A. Moiola, “A note on properties of the restriction operator on sobolev spaces,” *Journal of Applied Analysis*, vol. 23, no. 1, pp. 1–8, 2017.
- [11] G. Geymonat, “Trace theorems for sobolev spaces on lipschitz domains. necessary conditions,” in *Annales mathématiques Blaise Pascal*, vol. 14, no. 2, 2007, pp. 187–197.

- [12] J. Necas, *Direct methods in the theory of elliptic equations*. Springer Science & Business Media, 2011.
- [13] G. Chen and J. Zhou, *Boundary element methods with applications to nonlinear problems*. Springer Science & Business Media, 2010, vol. 7.
- [14] L. Hörmander, *The analysis of linear partial differential operators I: Distribution theory and Fourier analysis*. Springer, 2015.
- [15] L. C. Evans and R. F. Gariepy, *Measure theory and fine properties of functions*. CRC press, 2015.
- [16] R. Courant and D. Hilbert, *Methods of mathematical physics: partial differential equations*. John Wiley & Sons, 2008.
- [17] D. Borthwick, *Spectral Theory: Basic Concepts and Applications*. Springer Nature, 2020, vol. 284.
- [18] M. Reed and B. Simon, *II: Fourier Analysis, Self-Adjointness*. Elsevier, 1975, vol. 2.
- [19] P. Freitas and D. Krejčířík, “A sharp upper bound for the first dirichlet eigenvalue and the growth of the isoperimetric constant of convex domains,” *Proceedings of the American Mathematical Society*, vol. 136, no. 8, pp. 2997–3006, 2008.
- [20] D. Bucur, “Minimization of the k-th eigenvalue of the dirichlet laplacian,” *Archive for Rational Mechanics and Analysis*, vol. 206, no. 3, pp. 1073–1083, 2012.
- [21] J. Gómez-Serrano and G. Orriols, “Any three eigenvalues do not determine a triangle,” *Journal of Differential Equations*, vol. 275, pp. 920–938, 2021.
- [22] P. R. Antunes and P. Freitas, “On the inverse spectral problem for euclidean triangles,” *Proceedings of the Royal Society A: Mathematical, Physical and Engineering Sciences*, vol. 467, no. 2130, pp. 1546–1562, 2011.
- [23] M. Kac, “Can one hear the shape of a drum?” *The american mathematical monthly*, vol. 73, no. 4P2, pp. 1–23, 1966.
- [24] C. Gordon, D. Webb, and S. Wolpert, “Isospectral plane domains and surfaces via riemannian orbifolds,” *Inventiones mathematicae*, vol. 110, no. 1, pp. 1–22, 1992.
- [25] P. A. M. Dirac, “The quantum theory of the electron,” *Proceedings of the Royal Society of London. Series A, Containing Papers of a Mathematical and Physical Character*, vol. 117, no. 778, pp. 610–624, 1928.
- [26] P. Briet and D. Krejčířík, “Spectral optimization of dirac rectangles,” *Journal of Mathematical Physics*, vol. 63, no. 1, p. 013502, 2022.

- [27] T. Vu, "Spectral inequality for dirac right triangles," *arXiv preprint arXiv:2302.13040*, 2023.
- [28] D. Krejcirik, S. Larson, and V. Lotoreichik, "Problem list of the aim workshop," 2019. [Online]. Available: <http://aimpl.org/shapesurface/>
- [29] R. D. Benguria, S. Fournais, E. Stockmeyer, and H. Van Den Bosch, "Spectral gaps of dirac operators describing graphene quantum dots," *Mathematical Physics, Analysis and Geometry*, vol. 20, pp. 1–12, 2017.
- [30] V. Lotoreichik and T. Ourmières-Bonafos, "A sharp upper bound on the spectral gap for graphene quantum dots," *Mathematical Physics, Analysis and Geometry*, vol. 22, pp. 1–30, 2019.
- [31] A. Quarteroni and A. Valli, *Domain decomposition methods for partial differential equations*. Oxford University Press, 1999, no. BOOK.
- [32] R. A. Adams and J. J. Fournier, *Sobolev spaces*. Elsevier, 2003.
- [33] S. Salsa, *Partial differential equations in action: from modelling to theory*. Springer, 2016, vol. 99.
- [34] F. Sauvigny, *Partial Differential Equations 1: Foundations and Integral Representations*. Springer Science & Business Media, 2012.
- [35] C. J. Alves, "On the choice of source points in the method of fundamental solutions," *Engineering Analysis with Boundary Elements*, vol. 33, no. 12, pp. 1348–1361, 2009.
- [36] R. Narasimhan and Y. Nievergelt, *Complex analysis in one variable*. Springer Science & Business Media, 2012.
- [37] R. Kress, *Linear Integral Equations*, ser. Applied Mathematical Sciences. Springer New York, 2013.
- [38] D. Colton and R. Kress, *Integral equation methods in scattering theory*. SIAM, 2013.
- [39] S. Valtchev, "Numerical analysis of methods with fundamental solutions for acoustic and elastic wave propagation problems," Ph.D. dissertation, Universidade Técnica de Lisboa, Instituto Superior Técnico, 2008.
- [40] C. Alves and C. Chen, "A new method of fundamental solutions applied to nonhomogeneous elliptic problems," *Advances in Computational Mathematics*, vol. 23, pp. 125–142, 2005.
- [41] S. Christiansen and E. Meister, "Condition number of matrices derived from two classes of integral equations," *Mathematical Methods in the Applied Sciences*, vol. 3, no. 1, pp. 364–392, 1981.
- [42] T. Kitagawa, "On the numerical stability of the method of fundamental solution applied to the dirichlet problem," *Japan Journal of Applied Mathematics*, vol. 5, pp. 123–133, 1988.

- [43] —, “Asymptotic stability of the fundamental solution method,” *Journal of Computational and Applied Mathematics*, vol. 38, no. 1-3, pp. 263–269, 1991.
- [44] A. H. Barnett and T. Betcke, “Stability and convergence of the method of fundamental solutions for helmholtz problems on analytic domains,” *Journal of Computational Physics*, vol. 227, no. 14, pp. 7003–7026, 2008.
- [45] C. J. Alves and P. R. Antunes, “The method of fundamental solutions applied to the calculation of eigenfrequencies and eigenmodes of 2d simply connected shapes,” *CMC-TECH SCIENCE PRESS*-, vol. 2, no. 4, p. 251, 2005.

Glossary

This document is incomplete. The external file associated with the glossary 'main' (which should be called `main.gls`) hasn't been created.

Check the contents of the file `main.gls`. If it's empty, that means you haven't indexed any of your entries in this glossary (using commands like `\gls` or `\glsadd`) so this list can't be generated. If the file isn't empty, the document build process hasn't been completed.

If you don't want this glossary, add `nomain` to your package option list when you load `glossaries-extra.sty`. For example:

```
\usepackage[nomain]{glossaries-extra}
```

Try one of the following:

- Add `automake` to your package option list when you load `glossaries-extra.sty`. For example:

```
\usepackage[automake]{glossaries-extra}
```

- Run the external (Lua) application:

```
makeglossaries-lite.lua "main"
```

- Run the external (Perl) application:

```
makeglossaries "main"
```

Then rerun \LaTeX on this document.

This message will be removed once the problem has been fixed.



Code of Project

Nulla dui purus, eleifend vel, consequat non, dictum porta, nulla. Duis ante mi, laoreet ut, commodo eleifend, cursus nec, lorem. Aenean eu est. Etiam imperdiet turpis. Praesent nec augue. Curabitur ligula quam, rutrum id, tempor sed, consequat ac, dui. Vestibulum accumsan eros nec magna. Vestibulum vitae dui. Vestibulum nec ligula et lorem consequat ullamcorper.

Listagem A.1: Example of a XML file.

```
1 <?xml version="1.0" encoding="UTF-8"?>
2 <StreamInfo version="2.0">
3   <Clip duration="PT01M0.00S">
4     <BaseURL>videos/</BaseURL>
5     <Description>svc_1</Description>
6     <Representation mimeType="video/SVC" codecs="svc" frameRate="30.00" bandwidth="401.90"
7       width="176" height="144" id="L0">
8       <BaseURL>svc_1</BaseURL>
9       <SegmentInfo from="0" to="11" duration="PT5.00S">
```

```

10         <BaseURL>svc_1-L0-</BaseURL>
11     </SegmentInfo>
12 </Representation>
13 <Representation mimeType="video/SVC" codecs="svc" frameRate="30.00" bandwidth="1322.60"
14     width="352" height="288" id="L1">
15     <BaseURL>svc_1/</BaseURL>
16     <SegmentInfo from="0" to="11" duration="PT5.00S">
17         <BaseURL>svc_1-L1-</BaseURL>
18     </SegmentInfo>
19 </Representation>
20 </Clip>
21 </StreamInfo>

```

Etiam imperdiet turpis. Praesent nec augue. Curabitur ligula quam, rutrum id, tempor sed, consequat ac, dui. Maecenas tincidunt velit quis orci. Sed in dui. Nullam ut mauris eu mi mollis luctus. Class aptent taciti sociosqu ad litora torquent per conubia nostra, per inceptos hymenaeos. Sed cursus cursus velit. Sed a massa. Duis dignissim euismod quam.

Listagem A.2: Assembler Main Code.

```

1  ; *****
2  ; * Constantes
3  ; *****
4
5  ON      EQU 1 ; contagem ligada
6  OFF     EQU 0 ; contagem desligada
7  INPUT   EQU 8000H ; endereço do porto de entrada
8          ;(bit 0 = RTC; bit 1 = botão)
9  OUTPUT  EQU 8000H ; endereço do porto de saída.
10
11
12 ; *****
13 ; * Stack
14 ; *****
15
16 PLACE   1000H
17 pilha:   TABLE 100H ; espaço reservado para a pilha
18 fim_pilha:
19
20 ; *****
21
22 PLACE   2000H
23
24 ; Tabela de vectores de interrupção
25
26 tab:     WORD    rot0
27
28 ; *****
29 ; * Programa Principal
30 ; *****
31
32 PLACE   0
33
34 inicio:
35     MOV BTE, tab ; incializa BTE
36     MOV R9, INPUT ; endereço do porto de entrada
37     MOV R10, OUTPUT ; endereço do porto de saída
38     MOV SP, fim_pilha
39     MOV R5, 1 ; inicializa estado do processo P1
40     MOV R6, 1 ; inicializa estado do processo P2
41     MOV R4, OFF ; inicializa controle de RTC
42     MOV R8, 0 ; inicializa contador
43     MOV R7, OFF ; inicialmente não permite contagem
44     EIO ; permite interrupções tipo 0

```



```

45     EI                ; activa interrupções
46
47 ciclo:
48     CALL P1           ; invoca processo P1
49     CALL P2           ; invoca processo P2
50     JMP  ciclo        ; repete ciclo
51
52 ; *****
53 ;* ROTINAS
54 ; *****
55
56 P1:
57     CMP R5, 1         ; se estado = 1
58     JZ  P1_1          ; se estado = 1
59     CMP R5, 2         ; se estado = 2
60     JZ  P1_2          ; se estado = 2
61 sai_P1:
62     RET              ; sai do processo.
63
64
65 P1_1:
66     MOVB R0, [R9]     ; lê porto de entrada
67     BIT R0, 1
68     JZ  sai_P1        ; se botão não carregado, sai do processo
69     MOV R7, ON        ; permite contagem do display
70     MOV R5, 2         ; passa ao estado 2 do P1
71     JMP sai_P1
72
73 P1_2:
74     MOVB R0, [R9]     ; lê porto de entrada
75     BIT R0, 1
76     JNZ sai_P1        ; se botão continua carregado, sai do processo
77     MOV R7, OFF       ; caso contrário, desliga contagem do display
78     MOV R5, 1         ; passa ao estado 1 do P1
79     JMP sai_P1

```

Class aptent taciti sociosqu ad litora torquent per conubia nostra, per inceptos hymenaeos. Phasellus eget nisl ut elit porta ullamcorper. Maecenas tincidunt velit quis orci. Sed in dui. Nullam ut mauris eu mi mollis luctus. Class aptent taciti sociosqu ad litora torquent per conubia nostra, per inceptos hymenaeos.

This inline MATLAB code `for i=1:3, disp('cool'); end;` uses the `\mcode{}` command.¹

Nullam ut mauris eu mi mollis luctus. Class aptent taciti sociosqu ad litora torquent per conubia nostra, per inceptos hymenaeos. Sed cursus cursus velit. Sed a massa. Duis dignissim euismod quam. Nullam euismod metus ut orci.

Listagem A.3: Matlab Function

```

1 for i = 1:3
2     if i >= 5 && a ~= b           % literate programming replacement
3         disp('cool');             % comment with some  $\pi x^2$ 
4     end
5     [i,ind] = max(vec);
6     x_last = x(1,end) - 1;
7     v(end);
8     ylabel('Voltage ( $\mu V$ )');
9 end

```

¹MATLAB Works also in footnotes: `for i=1:3, disp('cool'); end;`

Nullam ut mauris eu mi mollis luctus. Class aptent taciti sociosqu ad litora torquent per conubia nostra, per inceptos hymenaeos. Sed cursus cursus velit. Sed a massa. Duis dignissim euismod quam. Nullam euismod metus ut orci.

Listagem A.4: function.m

```
1 % Copyright 2010 The MathWorks, Inc.
2 function ObjTrack(position)
3 % #codegen
4 % First, setup the figure
5 numPts = 300;           % Process and plot 300 samples
6 figure;hold;grid;       % Prepare plot window
7 % Main loop
8 for idx = 1: numPts
9     z = position(:,idx); % Get the input data
10    y = kalmanfilter(z);  % Call Kalman filter to estimate the position
11    plot_trajectory(z,y); % Plot the results
12 end
13 hold;
14 end % of the function
```

Class aptent taciti sociosqu ad litora torquent per conubia nostra, per inceptos hymenaeos. Phasellus eget nisl ut elit porta ullamcorper. Maecenas tincidunt velit quis orci. Sed in dui. Nullam ut mauris eu mi mollis luctus. Class aptent taciti sociosqu ad litora torquent per conubia nostra, per inceptos hymenaeos. Sed cursus cursus velit. Sed a massa. Duis dignissim euismod quam. Nullam euismod metus ut orci. Vestibulum erat libero, scelerisque et, porttitor et, varius a, leo.

Listagem A.5: HTML with CSS Code

```
1 <!DOCTYPE html>
2 <html>
3   <head>
4     <title>Listings Style Test</title>
5     <meta charset="UTF-8">
6     <style>
7       /* CSS Test */
8       * {
9         padding: 0;
10        border: 0;
```

```

11     margin: 0;
12 }
13 </style>
14 <link rel="stylesheet" href="css/style.css" />
15 </head>
16 <header> hey </header>
17 <article> this is a article </article>
18 <body>
19     <!-- Paragraphs are fine -->
20     <div id="box">
21         <p>
22             Hello World
23         </p>
24         <p>Hello World</p>
25         <p id="test">Hello World</p>
26         <p></p>
27     </div>
28     <div>Test</div>
29     <!-- HTML script is not consistent -->
30     <script src="js/benchmark.js"></script>
31     <script>
32         function createSquare(x, y) {
33             // This is a comment.
34             var square = document.createElement('div');
35             square.style.width = square.style.height = '50px';
36             square.style.backgroundColor = 'blue';
37
38             /*
39              * This is another comment.
40              */
41             square.style.position = 'absolute';
42             square.style.left = x + 'px';
43             square.style.top = y + 'px';
44
45             var body = document.getElementsByTagName('body')[0];
46             body.appendChild(square);
47         };
48

```

```

49     // Please take a look at +=
50     window.addEventListener('mousedown', function(event) {
51         // German umlaut test: Berührungspunkt ermitteln
52         var x = event.touches[0].pageX;
53         var y = event.touches[0].pageY;
54         var lookAtThis += 1;
55     });
56     </script>
57 </body>
58 </html>

```

Nulla dui purus, eleifend vel, consequat non, dictum porta, nulla. Duis ante mi, laoreet ut, commodo eleifend, cursus nec, lorem. Aenean eu est. Etiam imperdiet turpis. Praesent nec augue. Curabitur ligula quam, rutrum id, tempor sed, consequat ac, dui. Vestibulum accumsan eros nec magna. Vestibulum vitae dui. Vestibulum nec ligula et lorem consequat ullamcorper.

Listagem A.6: HTML CSS Javascript Code

```

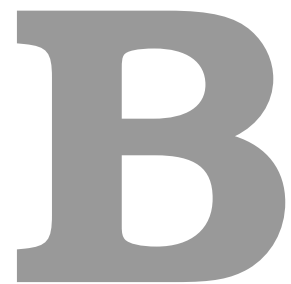
1
2 @media only screen and (min-width: 768px) and (max-width: 991px) {
3
4     #main {
5         width: 712px;
6         padding: 100px 28px 120px;
7     }
8
9     /* .mono {
10         font-size: 90%;
11     } */
12
13     .cssbtn a {
14         margin-top: 10px;
15         margin-bottom: 10px;
16         width: 60px;
17         height: 60px;
18         font-size: 28px;
19         line-height: 62px;
20     }

```

Nulla dui purus, eleifend vel, consequat non, dictum porta, nulla. Duis ante mi, laoreet ut, commodo eleifend, cursus nec, lorem. Aenean eu est. Etiam imperdiet turpis. Praesent nec augue. Curabitur ligula quam, rutrum id, tempor sed, consequat ac, dui. Vestibulum accumsan eros nec magna. Vestibulum vitae dui. Vestibulum nec ligula et lorem consequat ullamcorper.

Listagem A.7: PYTHON Code

```
1 class TelgramRequestHandler(object):
2     def handle(self):
3         addr = self.client_address[0]          # Client IP-address
4         telgram = self.request.recv(1024)      # Recieve telgram
5         print "From: %s, Received: %s" % (addr, telgram)
6         return
```

A Large Table

Aliquam et nisl vel ligula consectetur suscipit. Morbi euismod enim eget neque. Donec sagittis massa. Vestibulum quis augue sit amet ipsum laoreet pretium. Nulla facilisi. Duis tincidunt, felis et luctus placerat, ipsum libero vestibulum sem, vitae elementum wisi ipsum a metus. Nulla a enim sed dui hendrerit lobortis. Donec lacinia vulputate magna. Vivamus suscipit lectus at quam. In lectus est, viverra a, ultricies ut, pulvinar vitae, tellus. Donec et lectus et sem rutrum sodales. Morbi cursus. Aliquam a odio. Sed tortor velit, convallis eget, porta interdum, convallis sed, tortor. Phasellus ac libero a lorem auctor mattis. Lorem ipsum dolor sit amet, consectetur adipiscing elit.

Nunc auctor bibendum eros. Maecenas porta accumsan mauris. Etiam enim enim, elementum sed, bibendum quis, rhoncus non, metus. Fusce neque dolor, adipiscing sed, consectetur et, lacinia sit amet, quam. Suspendisse wisi quam, consectetur in, blandit sed, suscipit eu, eros. Etiam ligula enim, tempor ut, blandit nec, mollis eu, lectus. Nam cursus. Vivamus iaculis. Aenean risus purus, pharetra in, blandit quis, gravida a, turpis. Donec nisl. Aenean eget mi. Fusce mattis est id diam. Phasellus faucibus interdum sapien. Duis quis nunc. Sed enim. Nunc auctor bibendum eros. Maecenas porta accumsan mauris. Etiam enim enim, elementum sed, bibendum quis, rhoncus non, metus. Fusce neque dolor, adipiscing sed, consectetur et, lacinia sit amet, quam.

Table B.1: Example table

Benchmark: ANN	#Layers (1)	#Nets (2)	#Nodes* (3) = 8 · (1) · (2)	Critical path (4) = 4 · (1)	Latency (T_{iter}) (5)
A1	3–1501	1	24–12008	12–6004	4
A2	501	1	4008	2004	2–2000
A3	10	2–1024	160–81920	40	60 [†]
A4	10	50	4000	40	80–1200
Benchmark: FFT	FFT size [‡] (1)	#Inputs (2) = 2 ⁽¹⁾	#Nodes* (3) = 10 · (1) · (2)	Critical path (4) = 4 · (1)	Latency (T_{iter}) (5)
F1	1–10	2–1024	20–102400	4–40	6–60 [†]
F2	5	32	1600	20	40 – 1500
Benchmark: Random networks	#Types (1)	#Nodes (2)	#Networks (3)	Critical path (4)	Latency (T_{iter}) (5)
R1	3	10–2000	500	variable	(4)
R2	3	50	500	variable	(4) × [1; ⋯ ; 20]

* Excluding constant nodes.

[†] Value kept proportional to the critical path: (5) = (4) · 1.5.

[‡] A size of x corresponds to a 2^x point FFT.

Values in bold indicate the parameter being varied.

As Table B.1 shows, the data can be inserted from a file, in the case of a somehow complex structure. Notice the Table footnotes.

Lorem ipsum dolor sit amet, consectetur adipiscing elit. Morbi commodo, ipsum sed pharetra gravida, orci magna rhoncus neque, id pulvinar odio lorem non turpis. Nullam sit amet enim. Suspendisse id velit vitae ligula volutpat condimentum. Aliquam erat volutpat. Sed quis velit. Nulla facilisi. Nulla libero. Vivamus pharetra posuere sapien. Nam consectetur. Sed aliquam, nunc eget euismod ullamcorper, lectus nunc ullamcorper orci, fermentum bibendum enim nibh eget ipsum. Donec porttitor ligula eu dolor. Maecenas vitae nulla consequat libero cursus venenatis. Nam magna enim, accumsan eu, blandit sed, blandit a, eros.

And now an example (Table B.2) of a table that extends to more than one page. Notice the repetition of the Caption (with indication that is continued) and of the Header, as well as the continuation text at the bottom.

Table B.2: Example of a very long table spreading in several pages

Time (s)	Triple chosen	Other feasible triples
0	(1, 11, 13725)	(1, 12, 10980), (1, 13, 8235), (2, 2, 0), (3, 1, 0)
2745	(1, 12, 10980)	(1, 13, 8235), (2, 2, 0), (2, 3, 0), (3, 1, 0)
5490	(1, 12, 13725)	(2, 2, 2745), (2, 3, 0), (3, 1, 0)
8235	(1, 12, 16470)	(1, 13, 13725), (2, 2, 2745), (2, 3, 0), (3, 1, 0)
Continued on next page		

Table B.2 – continued from previous page

Time (s)	Triple chosen	Other feasible triples
10980	(1, 12, 16470)	(1, 13, 13725), (2, 2, 2745), (2, 3, 0), (3, 1, 0)
13725	(1, 12, 16470)	(1, 13, 13725), (2, 2, 2745), (2, 3, 0), (3, 1, 0)
16470	(1, 13, 16470)	(2, 2, 2745), (2, 3, 0), (3, 1, 0)
19215	(1, 12, 16470)	(1, 13, 13725), (2, 2, 2745), (2, 3, 0), (3, 1, 0)
21960	(1, 12, 16470)	(1, 13, 13725), (2, 2, 2745), (2, 3, 0), (3, 1, 0)
24705	(1, 12, 16470)	(1, 13, 13725), (2, 2, 2745), (2, 3, 0), (3, 1, 0)
27450	(1, 12, 16470)	(1, 13, 13725), (2, 2, 2745), (2, 3, 0), (3, 1, 0)
30195	(2, 2, 2745)	(2, 3, 0), (3, 1, 0)
32940	(1, 13, 16470)	(2, 2, 2745), (2, 3, 0), (3, 1, 0)
35685	(1, 13, 13725)	(2, 2, 2745), (2, 3, 0), (3, 1, 0)
38430	(1, 13, 10980)	(2, 2, 2745), (2, 3, 0), (3, 1, 0)
41175	(1, 12, 13725)	(1, 13, 10980), (2, 2, 2745), (2, 3, 0), (3, 1, 0)
43920	(1, 13, 10980)	(2, 2, 2745), (2, 3, 0), (3, 1, 0)
46665	(2, 2, 2745)	(2, 3, 0), (3, 1, 0)
49410	(2, 2, 2745)	(2, 3, 0), (3, 1, 0)
52155	(1, 12, 16470)	(1, 13, 13725), (2, 2, 2745), (2, 3, 0), (3, 1, 0)
54900	(1, 13, 13725)	(2, 2, 2745), (2, 3, 0), (3, 1, 0)
57645	(1, 13, 13725)	(2, 2, 2745), (2, 3, 0), (3, 1, 0)
60390	(1, 12, 13725)	(2, 2, 2745), (2, 3, 0), (3, 1, 0)
63135	(1, 13, 16470)	(2, 2, 2745), (2, 3, 0), (3, 1, 0)
65880	(1, 13, 16470)	(2, 2, 2745), (2, 3, 0), (3, 1, 0)
68625	(2, 2, 2745)	(2, 3, 0), (3, 1, 0)
71370	(1, 13, 13725)	(2, 2, 2745), (2, 3, 0), (3, 1, 0)
74115	(1, 12, 13725)	(2, 2, 2745), (2, 3, 0), (3, 1, 0)
76860	(1, 13, 13725)	(2, 2, 2745), (2, 3, 0), (3, 1, 0)
79605	(1, 13, 13725)	(2, 2, 2745), (2, 3, 0), (3, 1, 0)
82350	(1, 12, 13725)	(2, 2, 2745), (2, 3, 0), (3, 1, 0)
85095	(1, 12, 13725)	(1, 13, 10980), (2, 2, 2745), (2, 3, 0), (3, 1, 0)
87840	(1, 13, 16470)	(2, 2, 2745), (2, 3, 0), (3, 1, 0)
90585	(1, 13, 16470)	(2, 2, 2745), (2, 3, 0), (3, 1, 0)
93330	(1, 13, 13725)	(2, 2, 2745), (2, 3, 0), (3, 1, 0)
96075	(1, 13, 16470)	(2, 2, 2745), (2, 3, 0), (3, 1, 0)
98820	(1, 13, 16470)	(2, 2, 2745), (2, 3, 0), (3, 1, 0)
101565	(1, 13, 13725)	(2, 2, 2745), (2, 3, 0), (3, 1, 0)
104310	(1, 13, 16470)	(2, 2, 2745), (2, 3, 0), (3, 1, 0)
107055	(1, 13, 13725)	(2, 2, 2745), (2, 3, 0), (3, 1, 0)
109800	(1, 13, 13725)	(2, 2, 2745), (2, 3, 0), (3, 1, 0)
112545	(1, 12, 16470)	(1, 13, 13725), (2, 2, 2745), (2, 3, 0), (3, 1, 0)
115290	(1, 13, 16470)	(2, 2, 2745), (2, 3, 0), (3, 1, 0)
118035	(1, 13, 13725)	(2, 2, 2745), (2, 3, 0), (3, 1, 0)
120780	(1, 13, 16470)	(2, 2, 2745), (2, 3, 0), (3, 1, 0)
123525	(1, 13, 13725)	(2, 2, 2745), (2, 3, 0), (3, 1, 0)
126270	(1, 12, 16470)	(1, 13, 13725), (2, 2, 2745), (2, 3, 0), (3, 1, 0)
129015	(2, 2, 2745)	(2, 3, 0), (3, 1, 0)
131760	(2, 2, 2745)	(2, 3, 0), (3, 1, 0)
134505	(1, 13, 16470)	(2, 2, 2745), (2, 3, 0), (3, 1, 0)
137250	(1, 13, 13725)	(2, 2, 2745), (2, 3, 0), (3, 1, 0)
139995	(2, 2, 2745)	(2, 3, 0), (3, 1, 0)
142740	(2, 2, 2745)	(2, 3, 0), (3, 1, 0)
145485	(1, 12, 16470)	(1, 13, 13725), (2, 2, 2745), (2, 3, 0), (3, 1, 0)

Continued on next page

Table B.2 – continued from previous page

Time (s)	Triple chosen	Other feasible triples
148230	(2, 2, 2745)	(2, 3, 0), (3, 1, 0)
150975	(1, 13, 16470)	(2, 2, 2745), (2, 3, 0), (3, 1, 0)
153720	(1, 12, 13725)	(2, 2, 2745), (2, 3, 0), (3, 1, 0)
156465	(1, 13, 13725)	(2, 2, 2745), (2, 3, 0), (3, 1, 0)
159210	(1, 13, 13725)	(2, 2, 2745), (2, 3, 0), (3, 1, 0)
161955	(1, 13, 16470)	(2, 2, 2745), (2, 3, 0), (3, 1, 0)
164700	(1, 13, 13725)	(2, 2, 2745), (2, 3, 0), (3, 1, 0)

An example of a large Table that autofits the size to the page margins is illustrated in Table B.3. Please notice the text size that is shrunken in order for the table to adjust to the page:

Table B.3: Sample Table.

URL	First Time Visit	Last Time Visit	URL Counts	Value	Reference
https://web.facebook.com/	1521241972	1522351859	177	56640	[facebook-2021]
http://localhost/phpmyadmin/	1518413861	1522075694	24	39312	database-management
https://mail.google.com/mail/u/	1516596003	1522352010	36	33264	Google-Gmail-2021
https://github.com/shawon100	1517215489	1522352266	37	27528	Code-Repository
https://www.youtube.com/	1517229227	1521978502	24	14792	Youtube-video-2021

